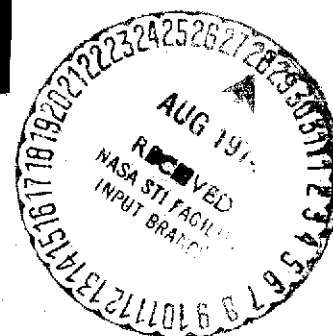


08

III



~~"Made available under NASA sponsorship
in the interest of early and wide dis-
semination of Earth Resources Survey
Program information and without liability
for any use made thereof."~~

Original photography may be purchased from
EROS Data Center
10th and Dakota Avenue
Sioux Falls, SD 57198

10604



THE UNIVERSITY OF KANSAS CENTER FOR RESEARCH, INC.

Space Technology Center—Nichols Hall
2291 Irving Hill Drive—Campus West
Lawrence, Kansas 66045

"Made available under NASA sponsorship
in the interest of early and wide dis-
semination of Earth Resources Survey
Program information and without liability
for any use made thereof."

E7.4-10714
CR-139553

KANSAS ENVIRONMENTAL AND
RESOURCE STUDY: A GREAT PLAINS
MODEL

MAY 1974

Type III Final Report for the
Period August 1, 1972 through May 15, 1974

STP

Original photography may be purchased from
EROS Data Center
10th and Dakota Avenue
Sioux Falls, SD 57198

Prepared for:

National Aeronautics and Space Administration
Goddard Space Flight Center
Greenbelt, Maryland 20771

Contract No. NAS 5-21822, Task 6



THE UNIVERSITY OF KANSAS CENTER FOR RESEARCH, INC.

2385 Irving Hill Rd.—Campus West Lawrence, Kansas 66044

RECEIVED

AUG 15 1974

SIS/902.6

KANSAS ENVIRONMENTAL AND RESOURCE STUDY:
A GREAT PLAINS MODEL

Ground Pattern Analysis in the Great Plains

F. T. Ulaby, Principal Investigator (Acting)
University of Kansas Center for Research, Inc.
Remote Sensing Laboratory
c/o Space Technology Center
Nichols Hall
2291 Irving Hill Drive-Campus West
Lawrence, Kansas 66045

(E74-10714) GROUND PATTERN ANALYSIS IN
THE GREAT PLAINS Final Report, 1 Aug.
1972 - 15 May 1974 (Kansas Univ. Center
for Research, Inc.) 84 p HC \$7.25

N74-31795

Unclas

CSCI 08B G3/13 00714

May 1974

Type III Final Report for the period August 1, 1972 through May 15, 1974
Report No. 2266-11

Original photography may be purchased from
EROS Data Center
10th and Dakota Avenue
Sioux Falls, SD 57198

Prepared for:

NATIONAL AERONAUTICS AND SPACE ADMINISTRATION
GODDARD SPACE FLIGHT CENTER
GREENBELT, MARYLAND 20771

Contract No. NAS 5-21822, Task 6

Final ERTS-A User
Investigation Report

Type III Final Report
for the Period August 1, 1972 through May 15, 1974

NASA Contract NAS 5-21822

Title of Investigation: Ground Pattern Analysis in the Great Plains

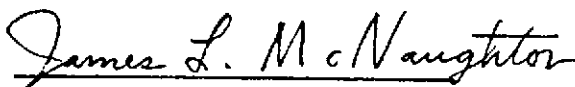
ERTS-A Proposal No.: 60-8

Task Number: 6

Co-principle Investigators: John C. Davis and Fawwaz T. Ulaby

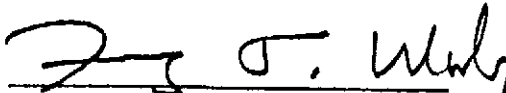
NASA-GSFC PI ID No.: UN 657

Report Prepared by:



James L. McNaughton
Research Engineer

Report Approved by:



Fawwaz T. Ulaby
Co-principle Investigator

TECHNICAL REPORT STANDARD TITLE PAGE

1. Report No. 2266-11	2. Government Accession No.	3. Recipient's Catalog No.
4. Title and Subtitle Kansas Environmental and Resource Study: A Great Plains Model		5. Report Date May 1974
Ground Pattern Analysis in the Great Plains		6. Performing Organization Code
7. Author(s) James L. McNaughton and Fawwaz T. Ulaby	8. Performing Organization Report No. 2266-11	
9. Performing Organization Name and Address University of Kansas Center for Research, Inc. c/o Space Technology Center 2291 Irving Hill Dr.-Campus West Lawrence, Kansas 66045		10. Work Unit No.
12. Sponsoring Agency Name and Address National Aeronautics and Space Administration Goddard Space Flight Center Greenbelt, Maryland 20771 G. R. Stonesifer, Code 430		11. Contract or Grant No. NAS 5-21822
15. Supplementary Notes None		13. Type of Report and Period Covered Type III Final Report for the period Aug. 1, 1972 to May 15, 1974
16. Abstract <p>The purpose of this investigation was to locate large-scale geologic ground patterns and anomalies in Kansas using Earth Resources Technology Satellite (ERTS-1) imagery and optical data processing techniques. ERTS-1 sample areas were chosen and used as the input to an optical data processing system. The optical processor forms the diffraction pattern of the sample area and quantitative information obtained from the diffraction pattern is used to characterize each sample area. This characterization of the ERTS sample areas is shown to work very well in discriminating between ground pattern categories in Kansas. The method of analysis used here is general and could be used to process various types of images.</p>		14. Sponsoring Agency Code
17. Key Words (Selected by Author(s)) Optical data processing; Diffraction pattern sampling; Spatial frequency analysis; Large-scale geologic ground pattern identification		18. Distribution Statement Original photography may be purchased from: EROS Data Center 10th and Dakota Avenue Sioux Falls, SD 57198
19. Security Classif. (of this report) Unclassified	20. Security Classif. (of this page) Unclassified	21. No. of Pages 75
		22. Price*

PREFACE

The objectives of this investigation are:

- A. Mapping the surficial geology of selected sites in Kansas from multispectral imagery, and identification of anomalous patterns;
- B. Search for large-scale ground patterns by spatial frequency analysis.

An optical processing system is used in this investigation to produce ground pattern spatial frequency and orientation information using ERTS-1 imagery as input. Interpretation of the information is done with respect to known geologic features and other cultural and vegetation features. Appropriate data processing schemes are used to derive numerical descriptors of these features and these descriptors, in turn, are used in pattern recognition schemes. This investigation will then provide a mapping technique of large-scale geologic ground patterns as well as other large-scale ground patterns in Kansas.

The manual interpretation of the spatial frequency and orientational information derived from the ERTS-1 imagery demonstrates that this information characterizes the sample areas very well. The results described here, based on this characterization of the sample areas, show that optical diffraction analysis can be used to accurately discriminate between large-scale ground patterns in Kansas.

TABLE OF CONTENTS

	<u>Page</u>
PREFACE	iii
LIST OF ILLUSTRATIONS	v
LIST OF TABLES	vii
1.0 INTRODUCTION	1
2.0 BACKGROUND	5
2.1 Theoretical Considerations	5
2.2 Other Investigations	8
3.0 EXPERIMENTAL ARRANGEMENT	9
3.1 Spatial Frequency Analysis of Sample Areas	9
3.2 Procedures and Measurements	12
3.2.1 Optical Processing System Description	12
3.2.2 Data Taking Procedure	15
3.3 Experimental Results	16
3.3.1 Analysis of Results for Sample Area Example	17
3.3.2 Examples of Results for the Eight Categories	20
3.3.3 Multispectral Example	24
4.0 CLASSIFICATION RESULTS AND ANALYSIS	27
4.1 Derivation of Pattern Descriptors (Parameters)	27
4.2 Physiographic Patterns Identified	32
4.3 Information Content of Frequency Bands	38
5.0 CONCLUSIONS	40
APPENDIX A- Optical Processor Equations	41
APPENDIX B- Equipment	44
APPENDIX C- Geology and Physiography of Kansas	46
APPENDIX D- Fortran IV Programs	53
REFERENCES	74

LIST OF ILLUSTRATIONS

<u>Figure</u>		<u>Page</u>
Figure 1.	Physiographic Regions of Kansas (Adapted from Schoewe, 1949) with Sample Site Location.	4
Figure 2.	Configuration Assumed for the Derivation of Equation 1.	6
Figure 3.	Block Diagram of Optical Processing and Pattern Recognition System.	10
Figure 4.	Detail of Portion of Fig. 3 Enclosed in Dashed Lines.	11
Figure 5.	System Configuration.	13
Figure 6.	Detector Geometry.	13
Figure 7.	Example Showing Progression of Steps From Portion of ERTS Image No. 1076-16393-5 (a); to Diffraction Pattern (b); to Digitized Computer Plots (c); to Modified Spatial Frequency Curve (d).	18
Figure 8.	(a) Sample Area F-4; (b) Optical Processor curves; (c) Modified Frequency curve.	21
Figure 9.	(a) Sample Area F-6; (b) Optical Processor curves; (c) Modified Frequency curve.	21
Figure 10.	(a) Sample Area 0-1; (b) Optical Processor curves; (c) Modified Frequency curve.	22
Figure 11.	(a) Sample Area 0-20; (b) Optical Processor curves; (c) Modified Frequency curve.	22
Figure 12.	(a) Sample Area G-5; (b) Optical Processor curves; (c) Modified Frequency curve.	23
Figure 13.	(a) Sample Area G-15; (b) Optical Processor curves; (c) Modified Frequency curve.	23
Figure 14.	Portions of ERTS-1 Images 1006-16502-4,5,6,7 and Optical Diffraction Curves for Sample M without Snow.	25
Figure 15.	Parameter Plot Using the Parameter (R) SLOPE 2.	29
Figure 16.	Parameter Plot Using the Parameter (R) SLOPE 2 for the Snow-covered Sample Areas.	30
Figure 17.	Parameter Plot Using the Parameter (R) DAV 1.	31

LIST OF ILLUSTRATIONS (Continued)

<u>Figure</u>		<u>Page</u>
Figure 18.	Classification of Sample Areas in Terms of a Decision Made on the Value of the Parameter SLOPE 2 for Each Sample Area.	33
Figure 19.	Scattergram Obtained Using the Parameters SLOPE 2 and DARAN 2.	34
Figure 20.	Classification of Samples Areas Based on Figure 19.	37
Figure 21.	Examples of the Modified Spatial Frequency Curves Showing the Curves in All Three Frequency Bands for Sample Areas G-5, F-6.	39
Figure A-1.	Configuration Assumed for the Derivation of Equation A-6.	41
Figure B-1.	Optical Processing Equipment.	44

LIST OF TABLES

<u>Table</u>		<u>Page</u>
Table 1.	Result of Classification of Sample Areas Based on Figure 19.	36
Table B-1.	Average Radii of Photodetector Annular Rings.	45

1.0 INTRODUCTION

The purpose of this investigation was to determine if spatial frequency analysis of Earth Resources Technology Satellite (ERTS-1) imagery could provide an unbiased means of estimating the character and nature of large-scale ground patterns in the image. Specifically, this investigation involved the determination of spatial frequency and orientational information from large-scale ground patterns in Kansas using ERTS-1 imagery as the input to an optical data processing system. Since the physiography and geology of Kansas is well-known, this method would provide an objective means of identifying and classifying ground patterns and locating anomalous patterns.

The optical processing system used in this investigation forms the diffraction pattern of the input image transparency and provides data on the spatial spectrum of the image. It will be shown in this paper that this spatial frequency analysis of ERTS-1 images provides an accurate and unbiased means of automatically identifying large-scale ground patterns in Kansas. It is anticipated that the equipment, procedures, and methods described in this paper could be applied in general to obtain automatic pattern recognition using various types of images.

This paper will describe the physiographic and geologic patterns that exist in Kansas; it will review the theory involved in diffraction pattern analysis; it will describe the optical processing system used in this investigation; it will review the spatial frequency and orientational information derived from this optical processor; it will state the accuracy with which these parameters predict the existence of large-scale ground patterns and anomalous patterns in Kansas; and finally, this paper will state some of the conclusions that can be made based on the results obtained during the course of this investigation.

The procedure followed during this investigation is outlined below:

- (1) Determine the number and extent of various geologic/physiographic regions in Kansas from known geologic/physiographic information.
- (2) Select an adequate number of sample areas within each region.
- (3) Investigate the effect of snow cover on the ability of ERTS-1 imagery to display physiographic information. (To study this effect, equivalent sample areas are chosen from imagery with and without snow cover.)

- (4) Obtain data from the optical processor for the given sample areas.
- (5) Determine features of the optical processor data which will allow the categorization of the sample areas.
- (6) Investigate the ability of optical processor data to provide reliable physiographic classification using different classification algorithms.
- (7) Investigate the information content of various spatial frequency bands with respect to the investigation in (6) above.

Eight regions of Kansas were chosen as most representative of certain distinctive physiographic/geologic provinces. Ten sample areas were chosen from each of these regions. Each sample area is circular with a diameter of approximately 37 kilometers. Optical processor data were taken twice for each of these sample areas--once using an image when the area was snow-covered and once again using an image from the area when it was not snow-covered.

Spatial frequency and orientational curves for 148 sample areas (80 non-snow and 68 snow samples) were obtained using the optical data processing system. Appropriate data processing schemes were used to derive numerical parameters from these curves, and these parameters are used as descriptors of the sample areas. These parameters were used to categorize the sample areas in terms of the different physiographic/geologic provinces previously chosen.

It should be noted that the sample area sites were chosen where stream patterns provide a good expression of the geology or physiography of the geologic/physiographic province. Stream patterns, with respect to the scale of this experiment, are numerous, however, so this restriction did not severely limit the choice of sample sites.

The images that were used in this experiment were obtained from NASA's ERTS-1 Multispectral Scanner (MSS) Subsystem. Each ERTS-1 image covers an area of approximately 100 by 100 nautical miles.

Categories and Sample Site Location

Eight Physiographic regions in Kansas are shown in Figure 1 as adapted from Schoewe (1949). Each physiographic region is also a region of characteristic geology since each region contains similar landforms caused by similar geomorphic processes and each region also contains outcrops of the same dominant lithology and the same geologic age. An important note with respect to this investigation is that, in general, the land-use for each region is the same. Hence, each sample site was chosen in a well-defined physiographic/geologic region of Kansas.

Ten sample areas were chosen in each of these categories and the sample area center points are also plotted in Figure 1 (Some sample areas are in or cross over into neighboring states but are still in the same geologic category). Each site has an alpha-numeric designation. F-1 refers to the first sample area in the Flint Hills; 0-6 refers to the sixth sample area in the Osage Plains; etc. When the image sample areas were analyzed with snow-cover they were assigned a number ten more than the non-snow number (0-6, no snow becomes 0-16, snow). The sample area in the High Plains region of Kansas designated "M" in Figure 1 was analyzed for all four MSS frequency bands (MSS 4, 5, 6, 7). This was done in order to determine the relative information content of each band. For all other sample areas, MSS band 5 (0.6-0.7 microns) 70 mm positive transparencies were used in the analysis. It was judged that band 5 images contain the most information with respect to the objectives of this investigation.

As mentioned previously, each sample area is approximately 37 kilometers in diameter and this diameter plus the size of the physiographic region controlled the spacing of the sample areas within each category. The sample areas were analyzed twice--once with snow cover and once without snow cover. Most of the non-snow samples were from images recorded in the summer and fall of 1972. The images for samples with snow-cover were recorded in the winter of 1972/1973. Only 68 of the 80 sample areas were analyzed with snow-cover, however, since cloud-free images were not available for 12 of the snow-covered sample areas.

Detailed analysis of each sample area was performed and the results of this analysis were presented in Ulaby et al. (1973). For a discussion of the physiography and geology of Kansas see Appendix C.

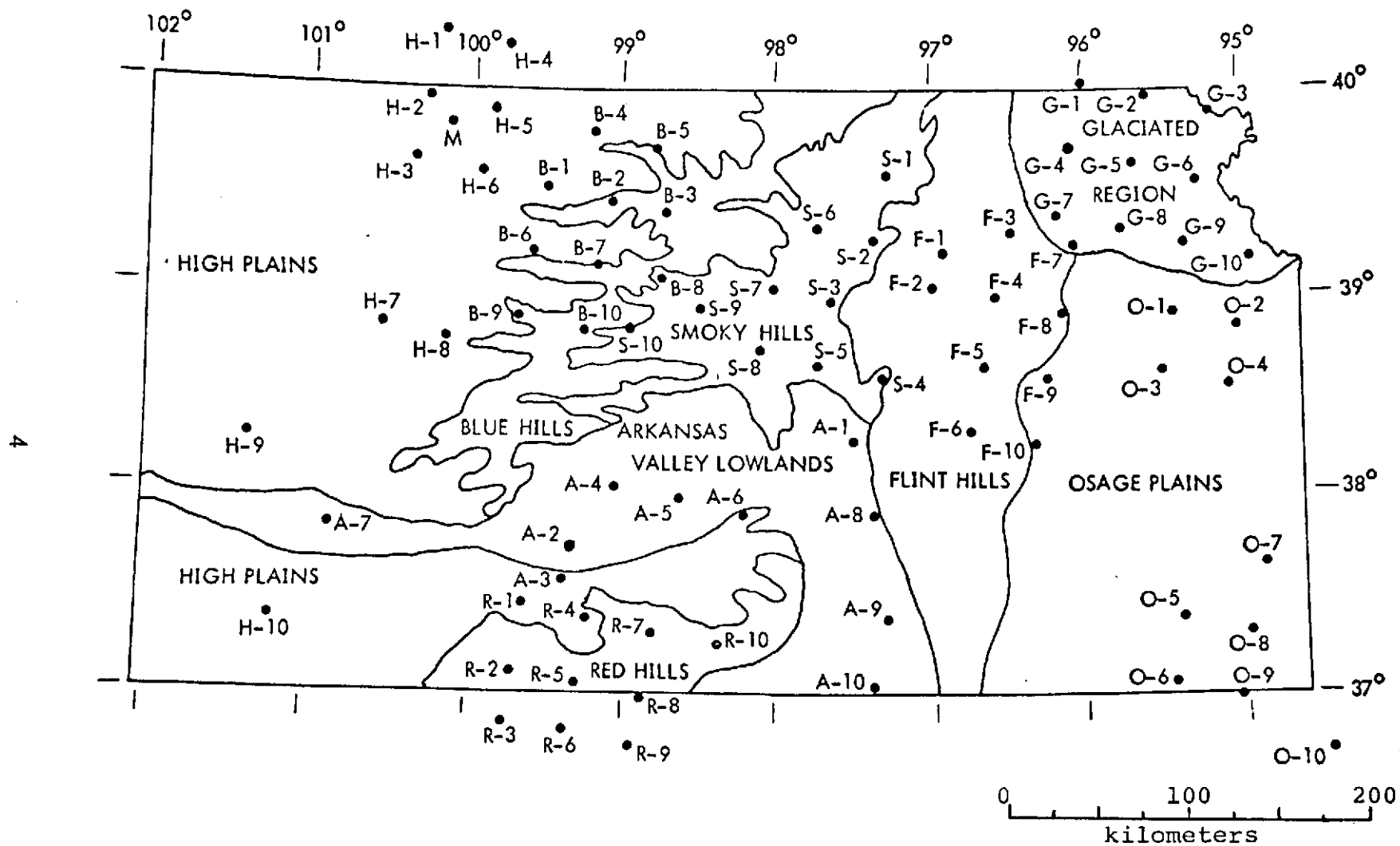


Figure 1. Physiographic Regions of Kansas (Adapted from Schoewe, 1949) with Sample Site Location.

2.0 BACKGROUND

2.1 Theoretical Considerations

This section is concerned with reviewing some of the theoretical background necessary to understand the basis of this investigation. The general area described here is referred to as optical data processing; the particular area with which this investigation is concerned is referred to as optical diffraction analysis or spatial frequency analysis. These terms arise because of the nature of the optical systems used.

The basic element needed to describe the nature of an optical data processing system for optical diffraction analysis or spatial frequency analysis is a single positive lens and an input object illuminated by an incident plane wave. From basic physical optics we know that a positive lens illuminated by an incident plane wave converts this wave into a wave converging upon a point f , where f is the focal point of the lens. The amazing aspect of this simple lens system is its ability to perform a two-dimensional Fourier transform.

If a plane object is inserted into this simple system at a point d_o away from the lens as shown in Figure 2, the distribution in the focal plane of the lens is proportional to the Fourier transform of the object's transmittance function (i.e. the complex function associated with the way in which the object transmits light). The illumination is assumed to be monochromatic and coherent.

In particular, if

$t_o(x,y)$ is the complex amplitude transmittance
function associated with the portion of
the object illuminated in Figure 2, and

$U_1(x_1,y_1)$ is the complex amplitude distribution
in the back focal plane of the lens, and

A is the amplitude of the normally incident
plane wave,

and assuming that the portion of the object illuminated is smaller in extent than the clear aperture of the lens we have (Goodman (1968)):

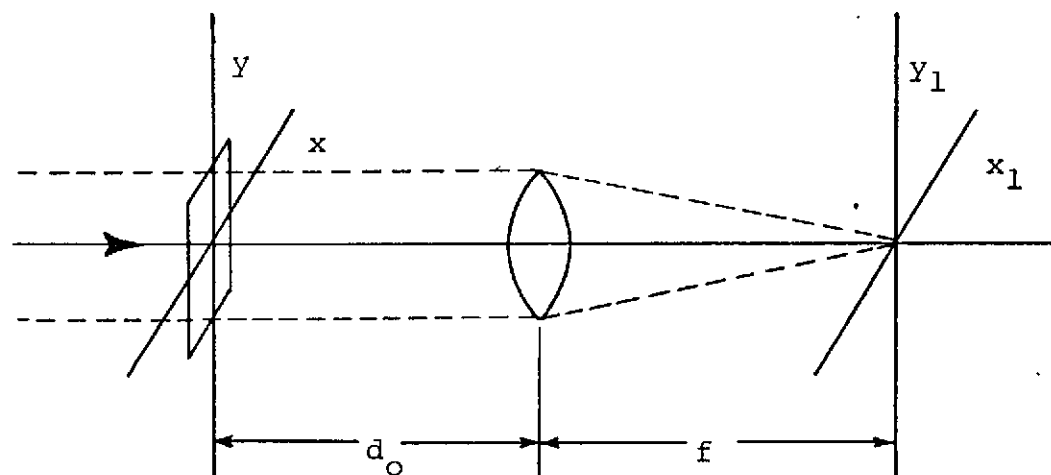


Figure 2. Configuration Assumed for the Derivation of Equation 1.

$$U_1(x_1, y_1) = B \iint_{-\infty}^{\infty} t_o(x, y) \exp \left[-j \frac{2\pi}{\lambda f} (xx_1 + yy_1) \right] dx dy \quad (1)$$

where

$$B = \frac{A}{j\lambda f} \exp \left[j \frac{k}{2f} \left(1 - \frac{d_o}{f} \right) (x_1^2 + y_1^2) \right]$$

Hence, the diffraction pattern in the back focal plane of the lens is proportional to the Fourier transform of the function which describes the object.

Note that the terms $x_1/f\lambda$ and $y_1/f\lambda$ in Equation (1) are scale factors relating the scale of the frequency distribution in the transform plane (back focal plane) to the scale of the distribution in the object plane. (i.e. for any point (x_1, y_1) in the transform plane, the spatial frequency associated with this point may be calculated from the geometry of the system to obtain the spatial frequency component values $(\frac{x_1}{f\lambda}, \frac{y_1}{f\lambda})$).

A mathematical description of the system used in this investigation is given in Appendix A. For a description of other optical processing configurations, the reader may consult Goodman (1968), Shulman (1970), or Preston (1972).

The distribution of interest has been described in terms of the Fourier transform of the input amplitude transmittance function. Hence, well-known theories from Fourier analysis can be applied in relating the transform to the original input (image transparency in this case).

Some of the aspects of Fourier analysis as applied to this investigation were presented in Ulaby et al. (1973) and McCauley et al. (1974). The basics of Fourier analysis can also be found in a number of textbooks dealing with advanced mathematics as well as in a number of electrical engineering texts dealing with the spectral analysis of signals.

2.2 Other Investigations

Basic physical optics and diffraction problems are discussed in Born and Wolf (1959), Goodman (1968), and Parrent and Thompson (1969). Optical systems similar to the one used in this investigation are discussed in Lee and Gossen (1971), and Read and Cannata (1974). Other current investigations which have used optical diffraction analysis for image analysis are: Stanley, Nienow and Lendaris (1969), and Lendaris and Stanley (1969), in which diffraction pattern sampling is used as a means to attain automatic target recognition; Davis and Preston (1972), McCullagh and Davis (1972), Pincus and Dobrin (1966), and Steckley (1972), in which optical diffraction analysis is used in geologic applications; and Read and Cannata (1974), in which one-dimensional data records are analyzed. Another investigation in which ERTS imagery is analyzed by diffraction pattern analysis is Gramenopoulos (1973). Two investigations which illustrate the technique of image processing by digital means are Haralick and Shanmugan (1973), and Andrews et al. (1972).

3.0 EXPERIMENTAL ARRANGEMENT

3.1 Spatial Frequency Analysis of Sample Areas

Each sample area on the ERTS image is composed of ground patterns of characteristic spatial frequencies and orientations. The spatial frequencies here refer to variations of density on the image as a function of distance. Hence, if we decompose the image sample area into its component frequencies and plot their intensity; and if we plot the 'strength' of preferred orientations in the image versus angle, we have described the sample area by a set of numbers. The purpose of the quantitative phase of this investigation was to determine how accurately this could be done.

The optical data processing system used in this investigation accomplishes this decomposition of the sample area in the manner described in section 2.1. A set of numbers is obtained which describe the spatial spectrum of the sample area and indicate the orientations of the large-scale ground patterns. Each of the sample areas on the ERTS images is used as the input to this optical processor.

A block diagram of the optical processing system along with the pattern recognition portion of the system is shown in Figure 3. Figure 4 expands on the part of Figure 3 enclosed in dashed lines. These diagrams show the various steps involved in going from the ERTS sample area to a categorization of the sample area based on the quantitative information derived from it.

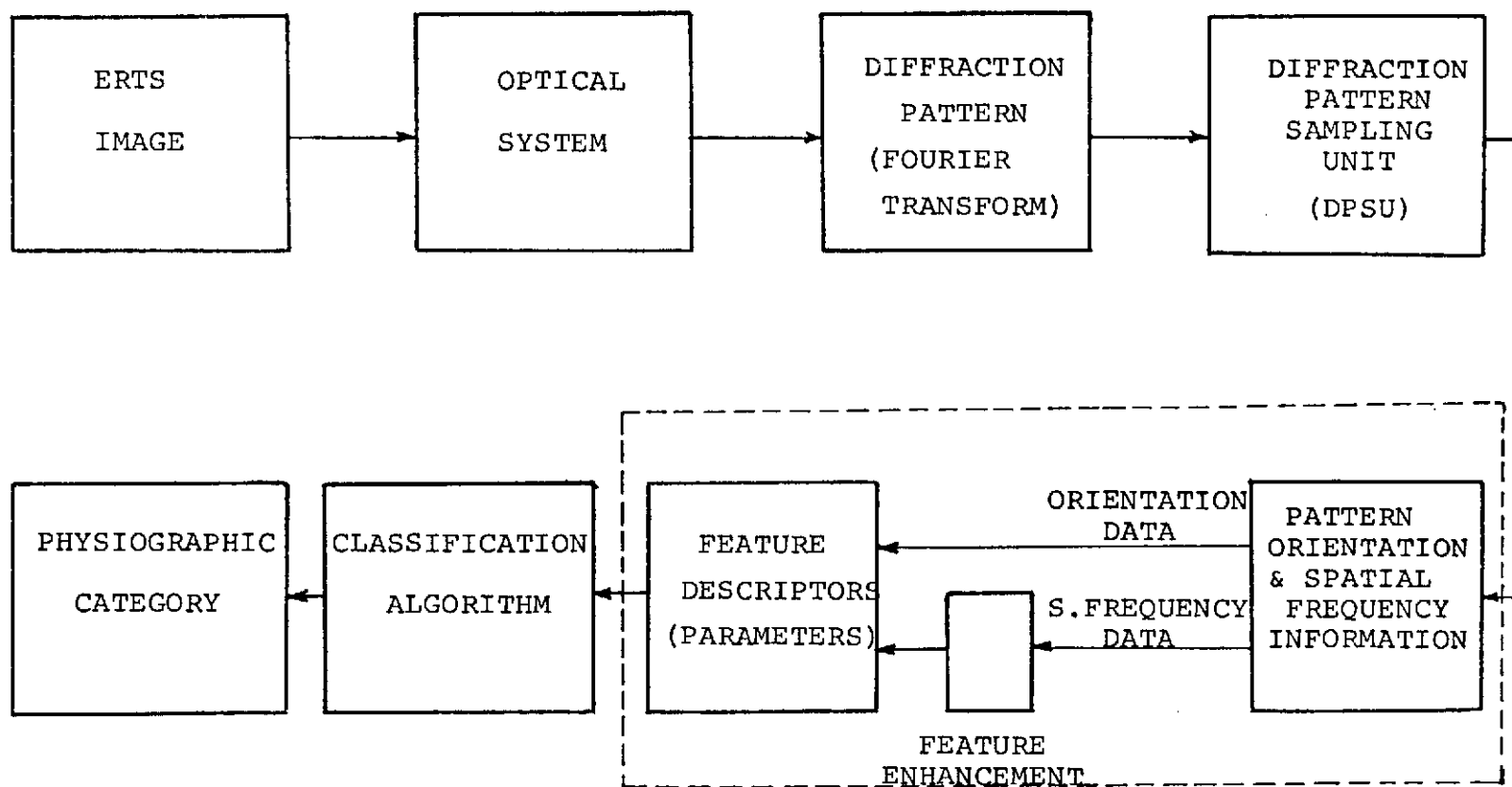


Figure 3 . Block diagram of optical processing and pattern recognition system.

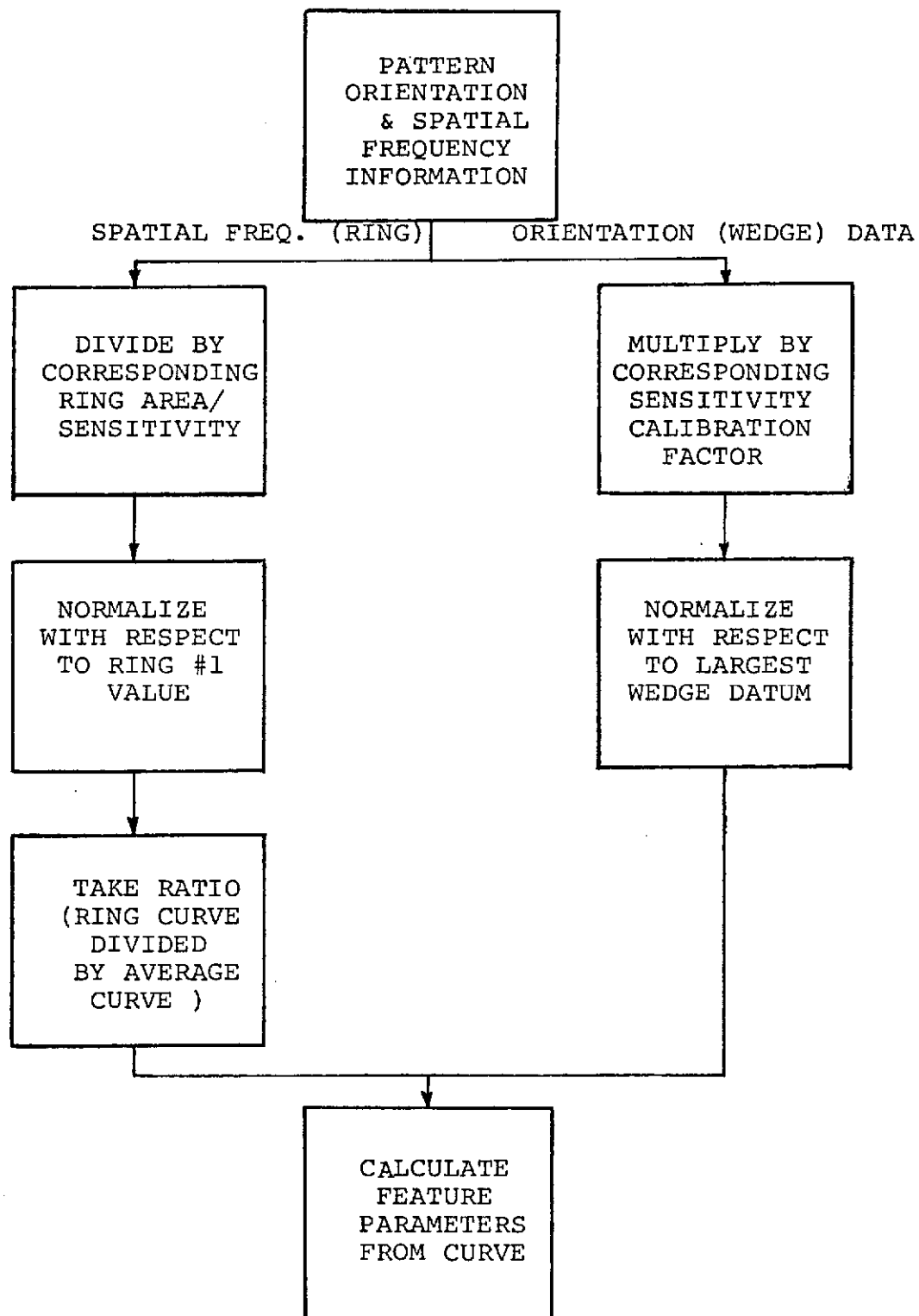


Figure 4. Detail of portion of Fig.3 enclosed in dashed lines.

3.2 Procedures and Measurements

3.2.1 Optical Processing System Description

In this section we will present a description of the optical processing system used for spatial frequency analysis of the ERTS images. The optical processor has three main elements: a laser, optics, and a Recognition Systems, Inc., Diffraction Pattern Sampling Unit (DPSU). The system configuration is shown in Figure 5. An ERTS-1 70 mm positive transparency is used as the input for this system. The optical processing system can be regarded as a two step system. First, an area of the ERTS transparency (sample area) is illuminated by the incident laser beam. This beam is focused by the lens so that the point source produced by the spatial filter is imaged at a distance $z + f$ in front of the lens. The light distribution in this plane is proportional to the Fourier transform of the transmittance function which describes the portion of the ERTS image illuminated by the beam. Second, the intensity distribution (spatial spectrum) of the ERTS image is sampled by the DPSU.

The DPSU consists of a 64 element photodiode array (shown in Figure 6) used to detect the light intensity incident upon each element, and electronics which amplify and digitize the output from each diode in the array. The diode array is composed of 32 wedge-shaped photodiodes and 32 annular ring photodiodes. The average intensity for each photodiode is recorded. These data are then used in a computer program and are calibrated, printed, and plotted.

The spatial frequency in the transform plane is related to other system parameters by:

$$s = r/d\lambda \quad (2)$$

where s = spatial frequency at a point r in the transform plane
 r = distance in transform plane measured from the optical axis
 d = distance from image transparency to detector
 λ = wavelength of laser radiation = 6328 Å

The spatial frequency from this calculation is converted to ground spatial frequency using image to ground scale. The resulting curves which are plotted by the computer program are then intensity vs. frequency and intensity vs. angle. These are plotted in terms of ground spatial frequency in cycles per kilometer and direction in compass degrees from north.

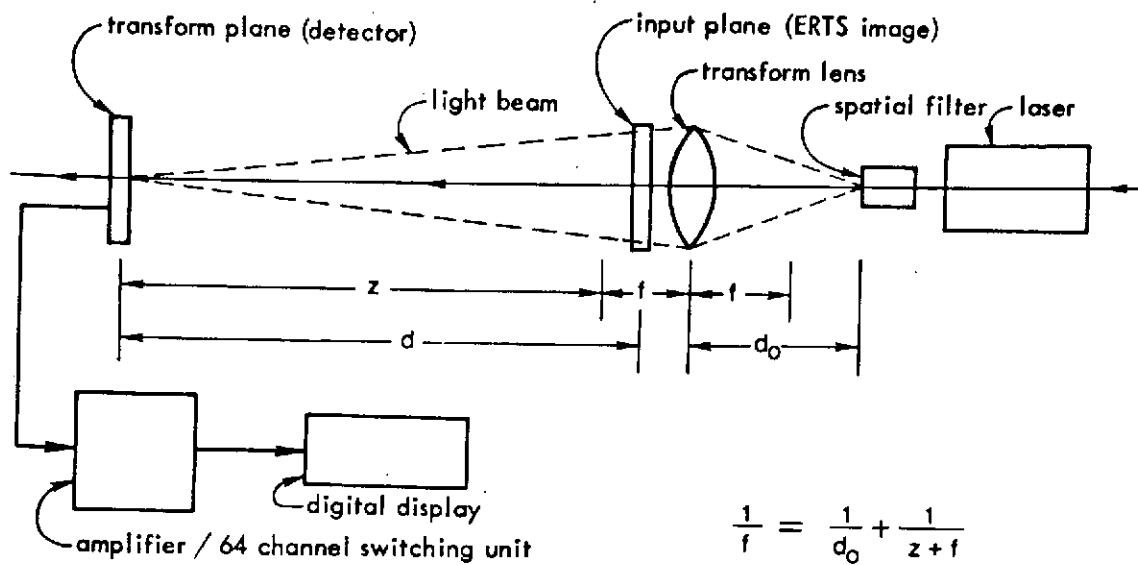


Figure 5. System Configuration

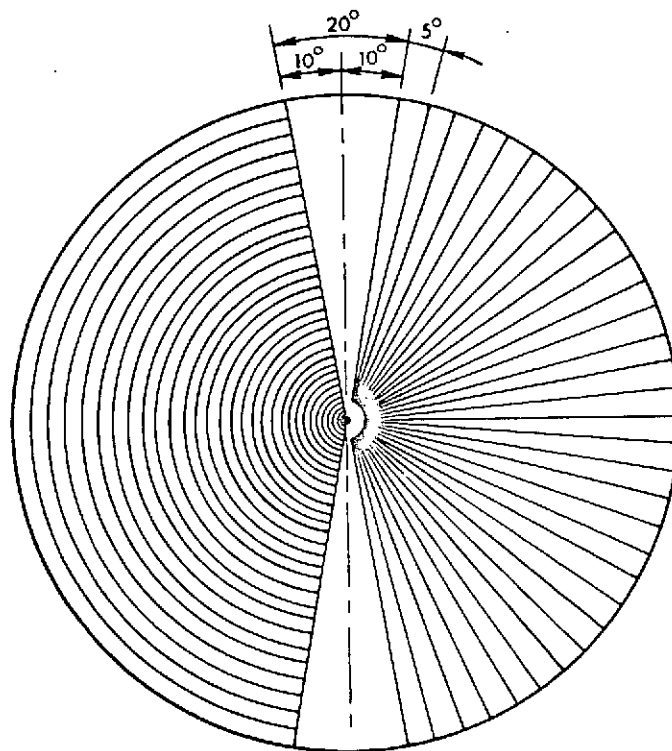


Figure 6. Detector Geometry

In order to calibrate the detector array, the array was illuminated with a uniform intensity, plane wave source. The intensity of the illumination was recorded for each element in the array and the measurements were used as the basis for the assignment of an area/sensitivity calibration factor to each element.

The mathematical description of this system is given in Appendix A.

3.2.2 Data Taking Procedure

The procedure used to record the data for each sample area is outlined below:

- (1) Set DPSU digital readout to zero. (Adjust 2nd Stage Balance Control - ring 30 switch on - set display = .000 at 1000 X gain.)
- (2) Place image on image holder. (image is aligned with respect to holder)
- (3) Choose sample area by moving ERTS image in image (x,y) plane. (The area on the ERTS image is chosen initially with respect to an x,y coordinate system.)
- (4) Align detector with respect to transform. (This is accomplished by moving the detector array in the transform plane with the center element (ring 1) switched into the circuit until the maximum reading is obtained on the digital display. This is a very critical adjustment that aligns the detector array with the optical axis of the system.)
- (5) Record data by switching each element of the array, in turn, into the circuit.
- (6) Enter data onto computer cards.
- (7) Run data calibration program. (Output is printed and automatically plotted.)

3.3 Experimental Results

The spatial frequency curves obtained for each sample area were modified to enhance their ability to display features of interest. An average spatial frequency curve was calculated for the 80 non-snow sample areas. The point-by-point ratio between this curve and each non-snow sample area frequency curve was determined and these values were plotted. A similar procedure was used for the snow sample area frequency curves. The relative amplitudes of the various frequency components are greatly emphasized using this method and it will be shown in the next chapter that these modified spatial frequency curves characterize the sample areas very well.

At this point in the analysis of the sample areas each sample has been described by a modified spatial frequency curve and an orientational curve. The steps involved in going from the ERTS sample areas to the modified spatial frequency and orientational curves are illustrated in the following section.

3.3.1 Analysis of Results for Sample Area Example

This section is intended to demonstrate how specific features in a sample area can be related to the spatial frequency and orientational information derived for it. Figure 7(a) shows a portion of ERTS-1 image no. 1076-16393-5. The circular area is sample area F-7 from the Flint Hills region of Kansas. 7(b) shows the diffraction pattern associated with the sample area shown in (a) as obtained with the optical processor. This pattern can be related to features in the sample area. The main feature of the diffraction pattern is the very bright distribution (labelled as A) extending vertically through the pattern. This distribution is due to the scan lines in the ERTS MSS images associated with the manner in which these images were obtained. Distributions which extend vertically in this manner are not detected with the DPSU, however, since a 20° dead space (see Fig. 6) exists in this region. It should be noted that because of the nature of the diffraction pattern, scan lines, which appear horizontally across the image, produce this vertical distribution. The intensity distribution in (b) is sampled using the DPSU described in the last section.

The normalized, calibrated spatial frequency (1) and orientational (2) curves are shown in Figure 7(c). As noted, these plots are obtained by recording the light intensity at each photodiode in the detector array and then using these data in a computer program. The spatial frequency curve, obtained from the ring-shaped photodiodes, gives the intensity of various spatial frequency components corresponding to features in the image sample area. The normalized intensity (shown here on a logarithmic scale) is recorded versus ground spatial frequency in cycles/kilometer. The orientational curve, obtained from the wedgeshaped photodiodes, indicate the orientation of features in the sample area. The normalized (with respect to the largest value) intensity is recorded versus the orientation clockwise in degrees from image north.

Figure 7(d) shows the modified spatial frequency curve obtained from the spatial frequency curve in (c). The amplitudes of the various frequency components are greatly emphasized in this modified frequency curve. The curve in (d) shows that frequency component values around .4 and 1.0 cycles/km tend to predominate. There are also peaks in the spatial frequency curve shown in (c) around .4 and 1.0 cycles/km. We would suspect that these peaks are caused by characteristic features in the sample area with these frequencies. The sample area in (a) shows that this is true. A band which is light in tone is apparent in this image. This band represents the Kansas River

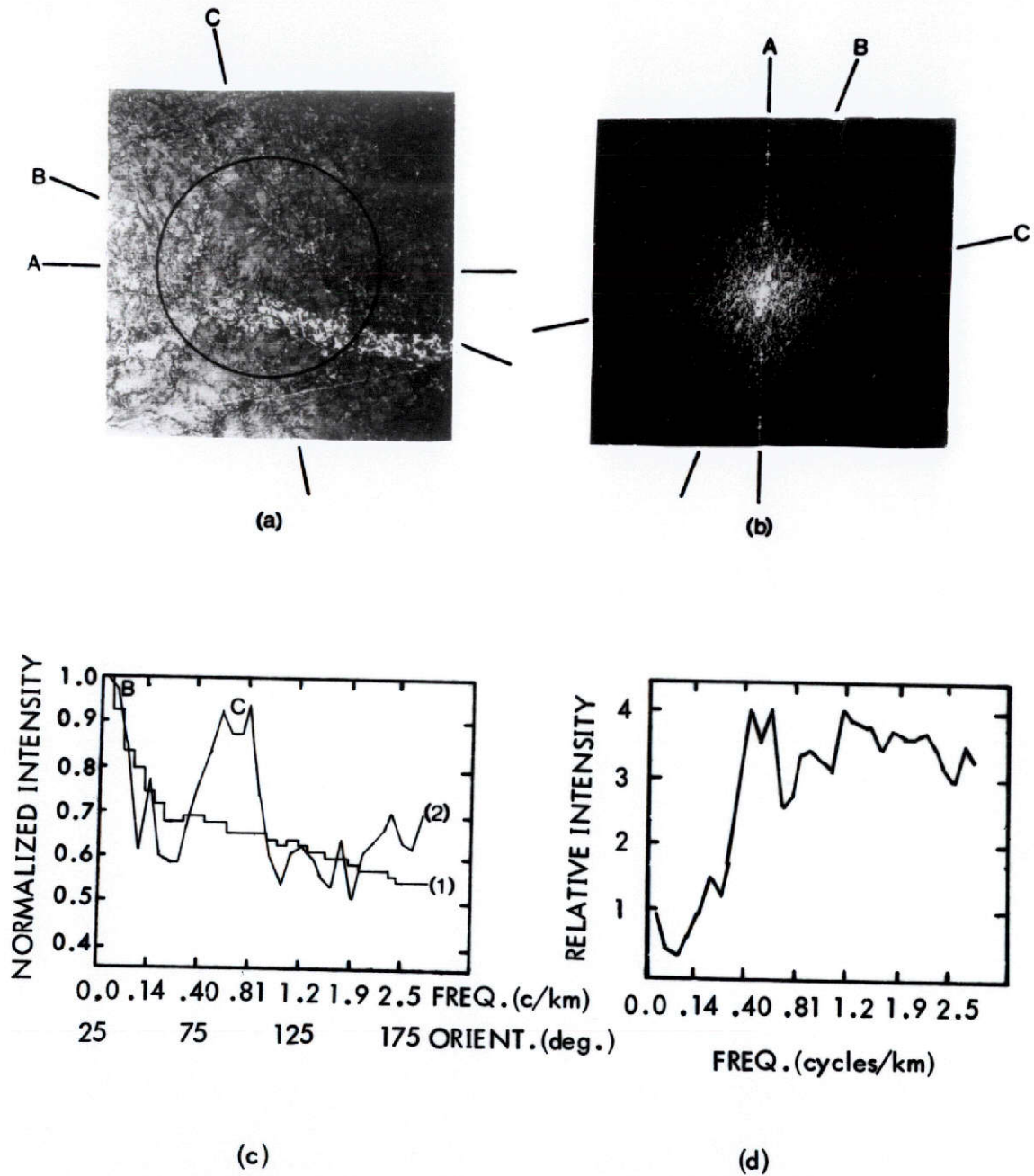


Figure 7. Example Showing Progression of Steps From Portion of ERTS Image No. 1076-16393-5 (a); to Diffraction Pattern (b); to Digitized Computer Plots (c); to Modified Spatial Frequency Curve (d).

flood plain which is an area of intensive agriculture. This band is approximately 2.5 kilometers wide and hence it has characteristic frequencies around $1/2.5 = 0.4$ cycles/km. The distribution around 1.0 is apparently produced by characteristic stream pattern frequencies. The orientational curve, curve (2) in 7 (c), also has a number of features which can be related to features in the sample area.

The two dominant peaks in this curve are labeled B and C. The peak at B, at approximately 35° , appears to result from the orientation of the Kansas River flood plain. This plain is oriented at approximately 30° to 35° clockwise from west in the sample area. Thus, because of the nature of the system, this plain produces the distribution at B in (b) which is oriented at 90° away. The peak at C in curve 2, 7(c) which occurs centered around 90° is due to the northward orientation of the field patterns and the general orientation of the major streams in the sample area. The distribution at C in (c) is also relatively wide indicating the variation in stream orientations around 90° . This example should illustrate how features in each sample area can be related to features in the diffraction pattern and in turn related to features in the spatial frequency and orientational curves.

3.3.2 Example of Results for the Eight Categories

Several of the ERTS sample areas are shown in Figures 8(a) through 13 (a). The resultant spatial frequency and orientational curves are shown in (b) for these areas, and the modified spatial frequency curves are shown in (c). (Peaks in the spatial frequency curves in (b) around .6 to .8 cycles/kilometer are usually caused by multiple scatter in ring 13 of the DPSU and hence are unrelated to image features.)

Figures 8(a) and 9(a) show two sample areas from the Flint Hills region of Kansas. Stream patterns in these two sample areas are well expressed and result in high peaks in the orientational curves in 8(b) and 9(b) corresponding to the orientation of the major streams. The modified frequency curves in 8(c) and 9(c) demonstrate characteristics of the modified frequency curves from the Flint Hills, the Blue Hills, and the Smoky Hills. The slope of these curves in the region beyond approximately 1.0 cycles/kilometer is positive and demonstrates the relatively larger high frequency content for sample areas from these categories.

Figures 10(a) and 11(a) show sample areas from the Osage Plains region where Figure 11(a) is a sample area with snow cover. There are numerous peaks in the orientational curves in 10(b) and 11(b) which is characteristic of orientational curves from sample areas from the Osage Plains. The modified frequency curves for both sample areas 10(a) and 11(a) fall off at higher frequencies in contrast to the curves in 8 (c) and 9 (c).

Figure 12 (a) shows sample area G-5 from the northeastern part of Kansas. The orientational curve in 12 (b) has high peaks at 90° and 180° indicating the dominant north-south, east-west orientation of the section roads and agricultural patterns in this area. Figure 13(a) shows the same sample area as in 12(a) with snow cover. The snow cover emphasizes the stream patterns in this case and the orientational curve, 13(b), has high peaks around 50° - 75° corresponding to the major stream orientations. The modified frequency curves shown in 12(c) and 13(c) again fall off at high frequencies.

These examples are intended to show how features in the spatial frequency and orientational curves can be used to categorize the sample areas. In chapter 4 it will be shown that features such as those shown here can be used to discriminate between various physiographic categories.

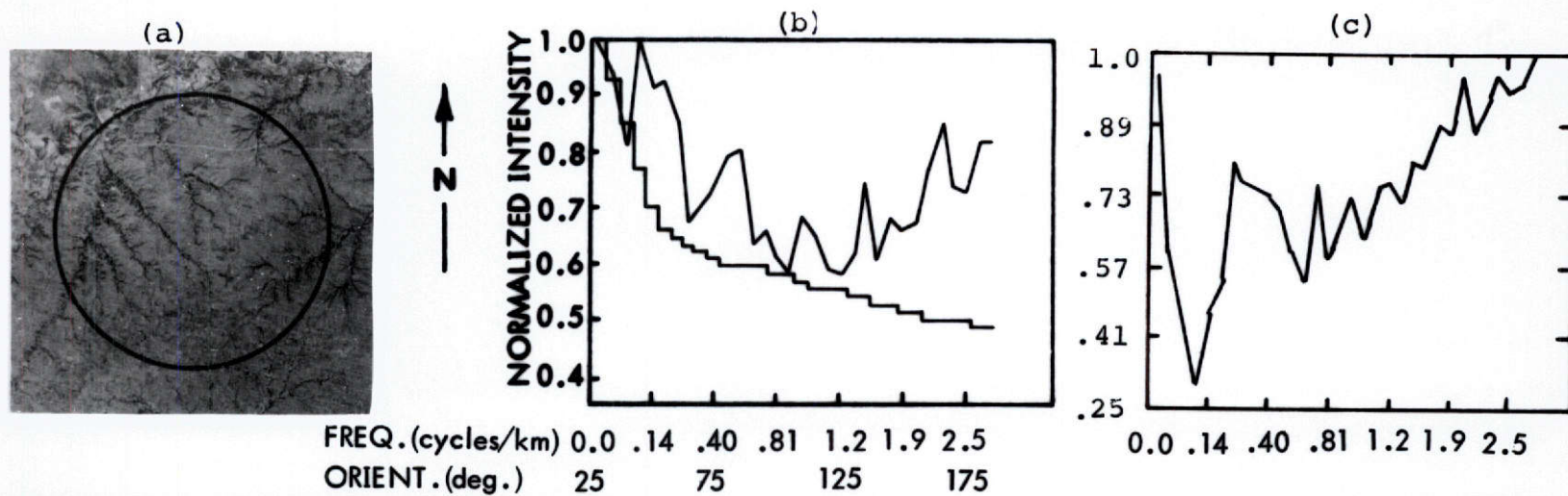


Figure 8. (a) Sample Area F-4; (b) Optical Processor Curves; (c) Modified Frequency Curve.

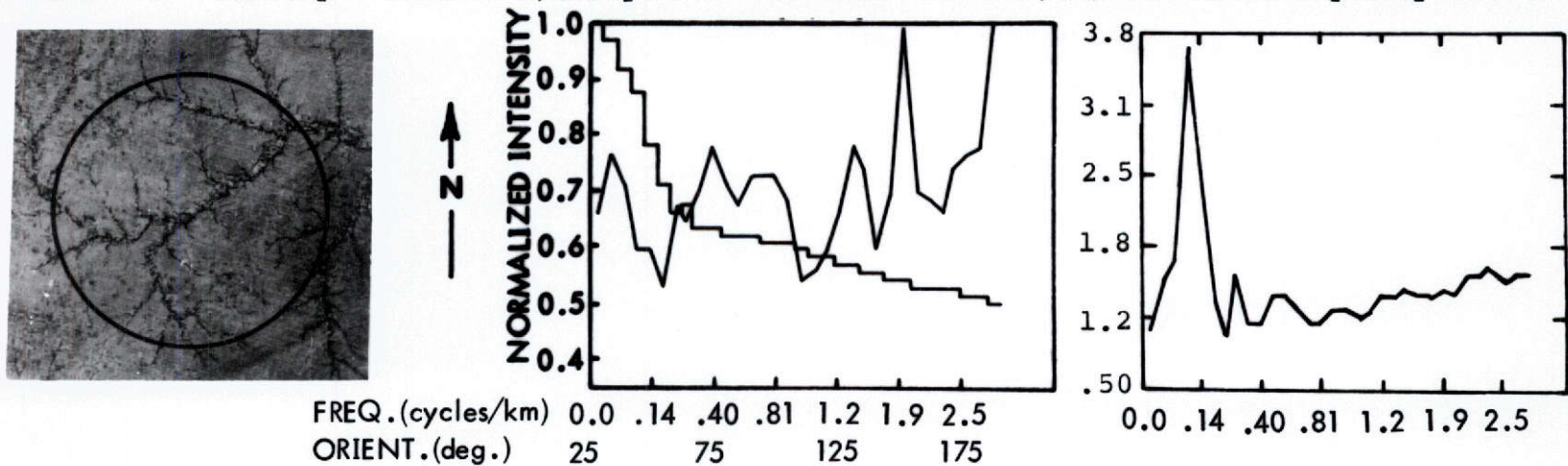


Figure 9. (a) Sample Area F-6; (b) Optical Processor Curves; (c) Modified Frequency Curve.

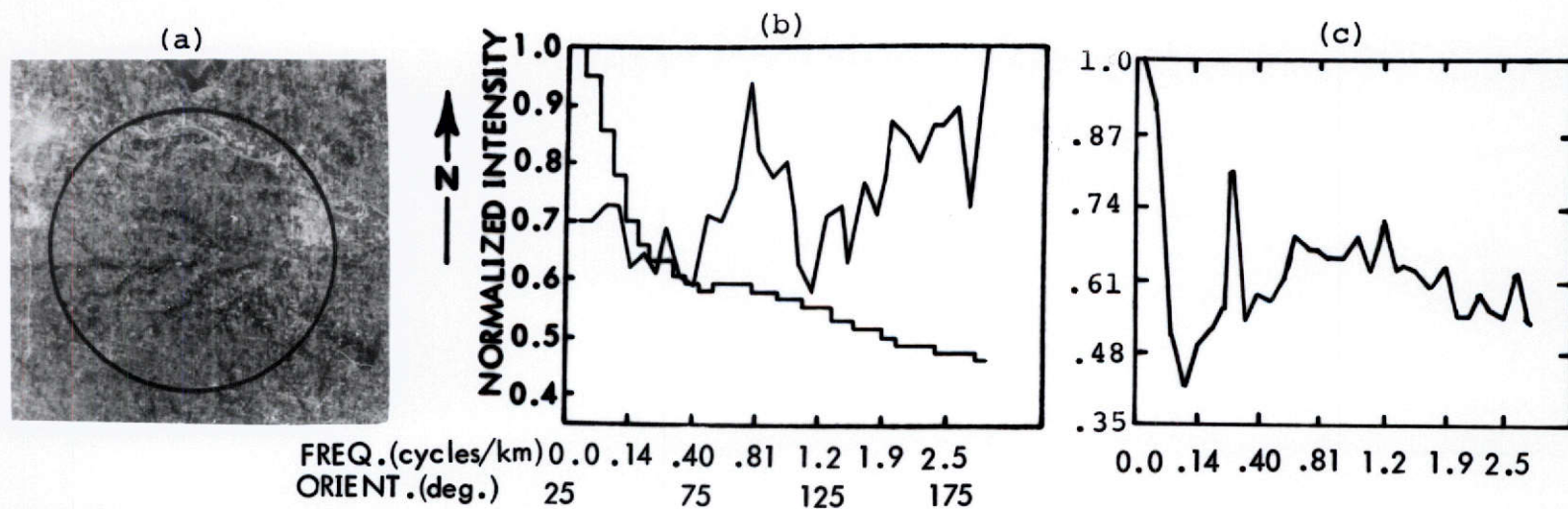


Figure 10. (a) Sample Area 0-1; (b) Optical Processor Curves; (c) Modified Frequency Curve.

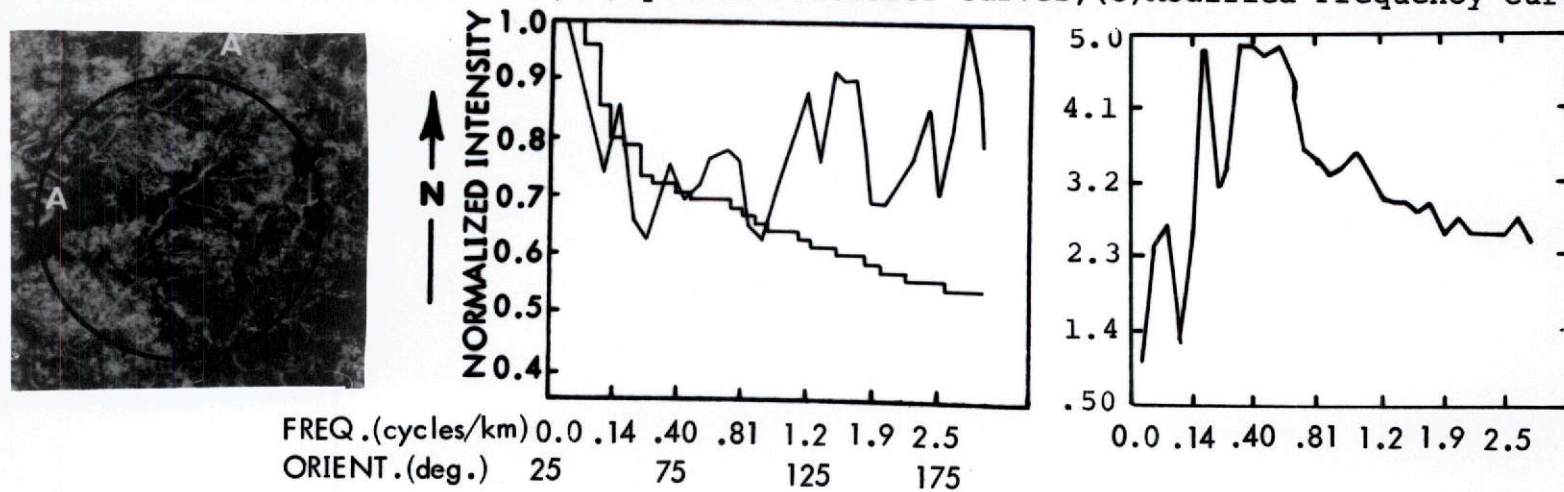


Figure 11. (a) Sample Area 0-20; (b) Optical Processor Curves; (c) Modified Frequency Curve.

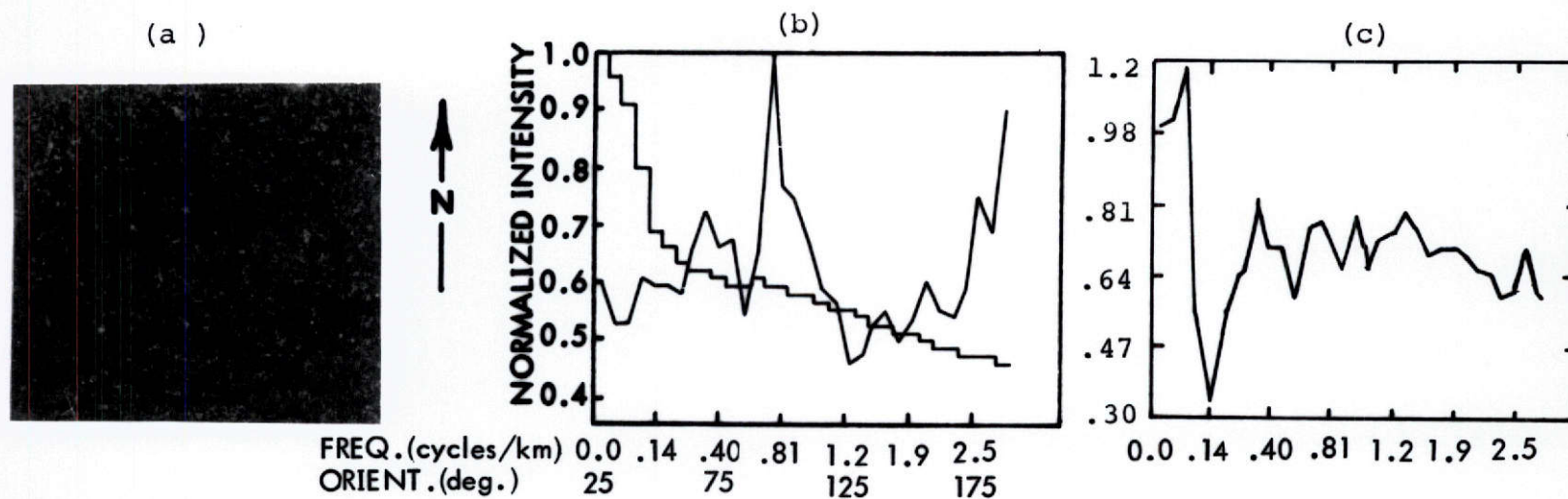


Figure 12. (a)Sample Area G-5; (b)Optical Processor Curves; (c)Modified Frequency Curve.

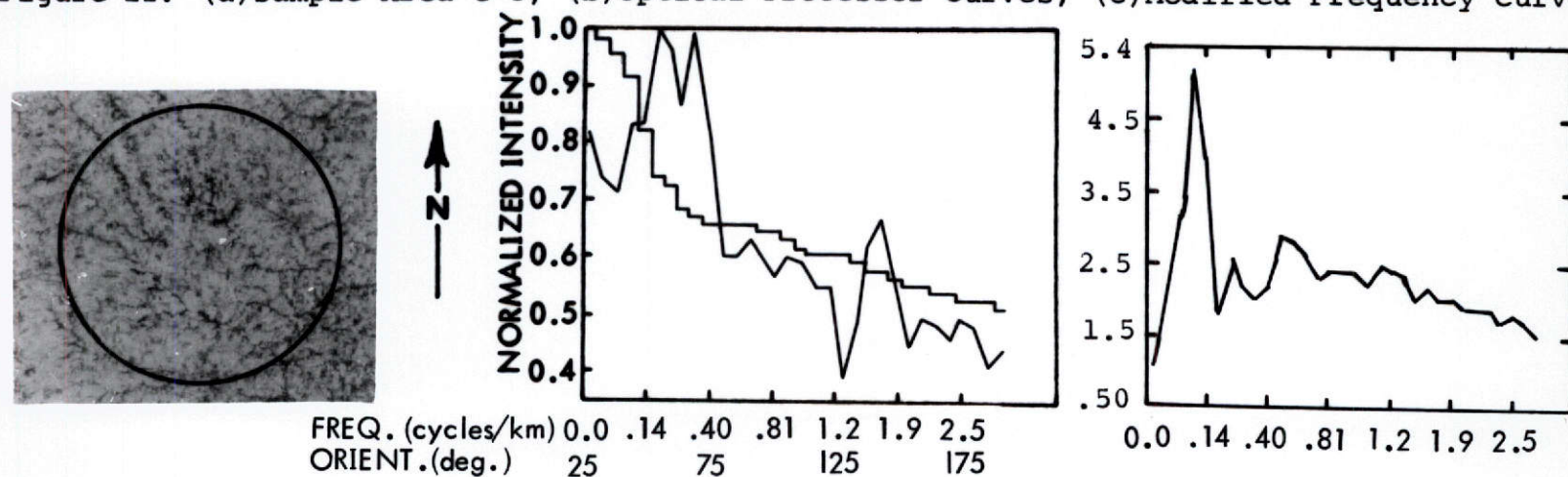


Figure 13. (a)Sample Area G-15; (b)Optical Processor Curves; (c)Modified Frequency Curve.

3.3.3 Multispectral Example

Figure 14 shows portions of ERTS-1 images 1006-16502-4,5,6,7 and the sample areas M-4, M-5, M-6 and M-7. The spatial frequency and orientational curves obtained with the optical data processing system are shown next to the respective samples. These images are from MSS bands 4(.5-.6 micrometers; 5(.6-.7 micrometers); 6(.7-.8 micrometers); and 7(.8-1.1 micrometers). The sample area shown here is in northwestern Kansas and contains a parallel drainage system which trends NW-SE. These four bands were analyzed in order to obtain quantitative information on the way in which features, specifically drainage patterns, are expressed in the various bands.

The expression of the drainage pattern in the four images for the four bands is a function of the land-use in this sample area from the High Plains region of Kansas. The rough stream valleys here are often used as pastureland and the level uplands are used for cultivation. The main feature that concerns us here is the difference in expression in the images between the grassy pastureland and the cultivated ground in the uplands. An idea of the relationship between the expression of the land-use categories in the images and the actual land-use can be obtained from curves of relative spectral radiance for various agricultural scenes. Curves of this type are shown in Remote Sensing (1970). Specifically, Figure 7, page 310 shows how the relative spectral radiance of four types of agricultural scenes changes as a function of wavelength. The main difference here is between the radiance of the various scenes in the visible and the infrared part of the spectrum. The curves shown in this figure demonstrate that the radiance of the grassy pastureland should be greater in the infrared bands than in the visible band and conversely, the radiance of the bare ground should be greater in the visible than in the infrared. This relationship is apparent in the image specifically where the drainage patterns are dark in tone in the visible bands (4 and 5), and are displayed as light in tone in the two infrared bands (6 and 7). Image features as they are displayed in the spatial frequency and orientational curves are described in the next paragraph.

The orientational curve for the band 4 image contains a peak at 100° which is due to the field patterns apparent in the image. The drainage pattern in this image is not enhanced as much as in the band 5 image due to the weaker reflectance of the field patterns in band 4. Because of the number of field patterns in the sample area,

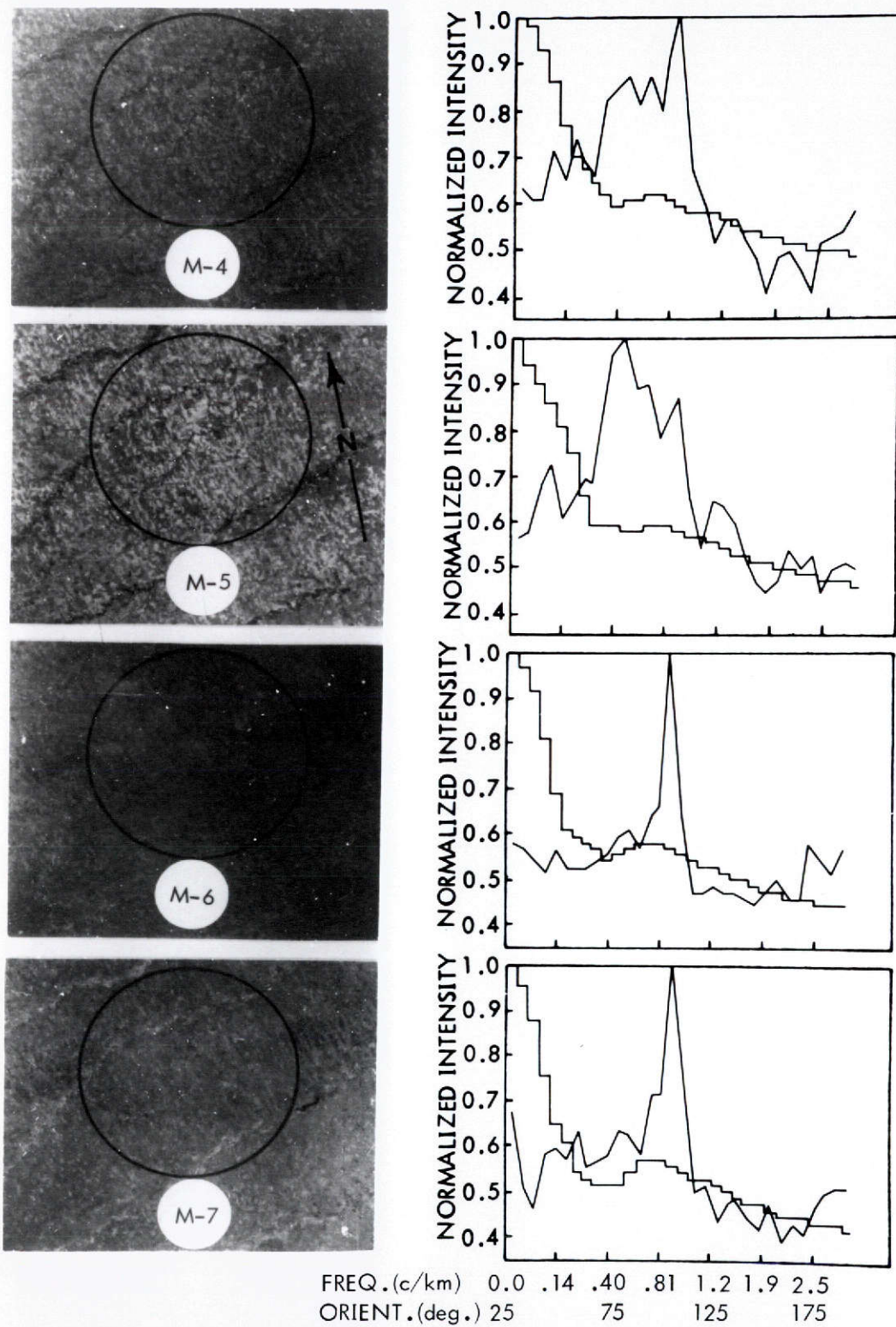


Figure 14 Portions of ERTS-1 Images 1006-16502-4,5,6,7 and Optical Diffraction Curves for Sample M without Snow.

the contribution due to the field patterns slightly dominates in the orientational curve. The parallel drainage pattern produces the secondary peaks at approximately 75° and 85° . The drainage pattern in the band 5 image is very apparent due to the enhancement effect provided by the field patterns. Correspondingly, the orientational curve displays the peak at 75° due to the drainage direction, and displays a secondary peak associated with the field patterns at 100° . The band 6 and band 7 images are similar and produce similar results. Both the drainage patterns and the field patterns appear to be subdued in these two images apparently because the medium reflectance of the fields again does not enhance the drainage patterns. Again because of the number of fields in the sample area, however, the orientational curves both have sharp peaks at 100° that result from these field patterns. The drainage pattern for both of these images does not contribute significantly to the orientational information displayed in the curve. The spatial frequency curves for all four images are similar. However, since features apparent in the sample area are delineated more sharply in the band 4 and band 5 images, the spatial frequency curves for these two bands do display a slightly greater high frequency content.

This example gives a quantitative view of why, in order to emphasize geologic ground features, band 5 images were chosen for analysis in this investigation.

4.0 CLASSIFICATION RESULTS AND ANALYSIS

4.1 Derivation of Pattern Descriptors

To reduce the amount of information present in the modified spatial frequency and orientational curves, various data processing schemes were developed to extract parameters from them. These parameters describe the geologic or physiographic features giving rise to fluctuations in the curves. To determine how well these parameters characterize each sample area, they may be used to categorize the sample areas by using the parameters as input to pattern classification algorithms.

The range of frequencies was divided into two bands. Band 1 contains spatial frequencies between 0.0 and 0.9 cycles/km and band 2 contains spatial frequencies between 1.1 and 2.8 cycles/km. This division essentially separates information due to high frequency fluctuations such as occur in stream patterns in rough terrain, and low frequency information such as occur due to field patterns. This division of frequencies appears to correspond to a natural break at approximately 1.0 cycles/km.

Similarly, the range of orientational data was divided into four sectors--each corresponding to 40 degrees (see Figure 6). Sector 1 provides data on pattern orientations that produce distributions between 25 and 65 degrees clockwise from north; sector 2: 65-105 degrees; sector 3: 105-145 degrees; and sector 4: 145-185 degrees.

Parameters are extracted from the spatial frequency and orientational curves in each range.

The following parameters were calculated from the spatial frequency and orientational curves in each of the bands or sectors listed above.

Orientalional Curve Parameters:

DAV	Average value of the curve in the 40° sector
RMSD	Root Mean Square Deviation of curve from overall average in each sector
AREA	A. Area of curve above overall average in sector B. Area of curve below overall average in sector
PEAK	Number of peaks or 'spikes' in curve in sector
PAKS	Number of data points above average in sector

Spatial Frequency Curve Parameters:

(These parameters are derived from the modified spatial frequency curve)

DAV	Average value of the curve in each frequency band
RMSD	Root Mean Square Deviation of curve from overall average in each band
AREA	A. Area of curve above overall average in band B. Area of curve below overall average in band
DARA	A. Area of curve above the value 1.0 in band B. Area of curve below the value 1.0 in band
DYNR	DYNAmic Range of curve in band
SLOPE 2	The slope of the regression line calculated for the curve in band 2

Each parameter for all 80 non-snow and 68 snow sample areas was plotted versus its appropriate sample area category as obtained from Figure 1. Three of these parameter plots are shown in Figures 15, 16, and 17. Two separate parameters are listed and one of these is repeated for the 68 snow sample areas. The notation 'R' or 'W' preceding the parameter name denotes the parameter as a spatial frequency (ring) or orientational (wedge) parameter respectively.

Figure 15. Parameter Plot Using the Parameter (R) SLOPE2.

Figure 16. Parameter Plot Using the Parameter (R)SLOPE2 for the Snow-covered Sample Areas.

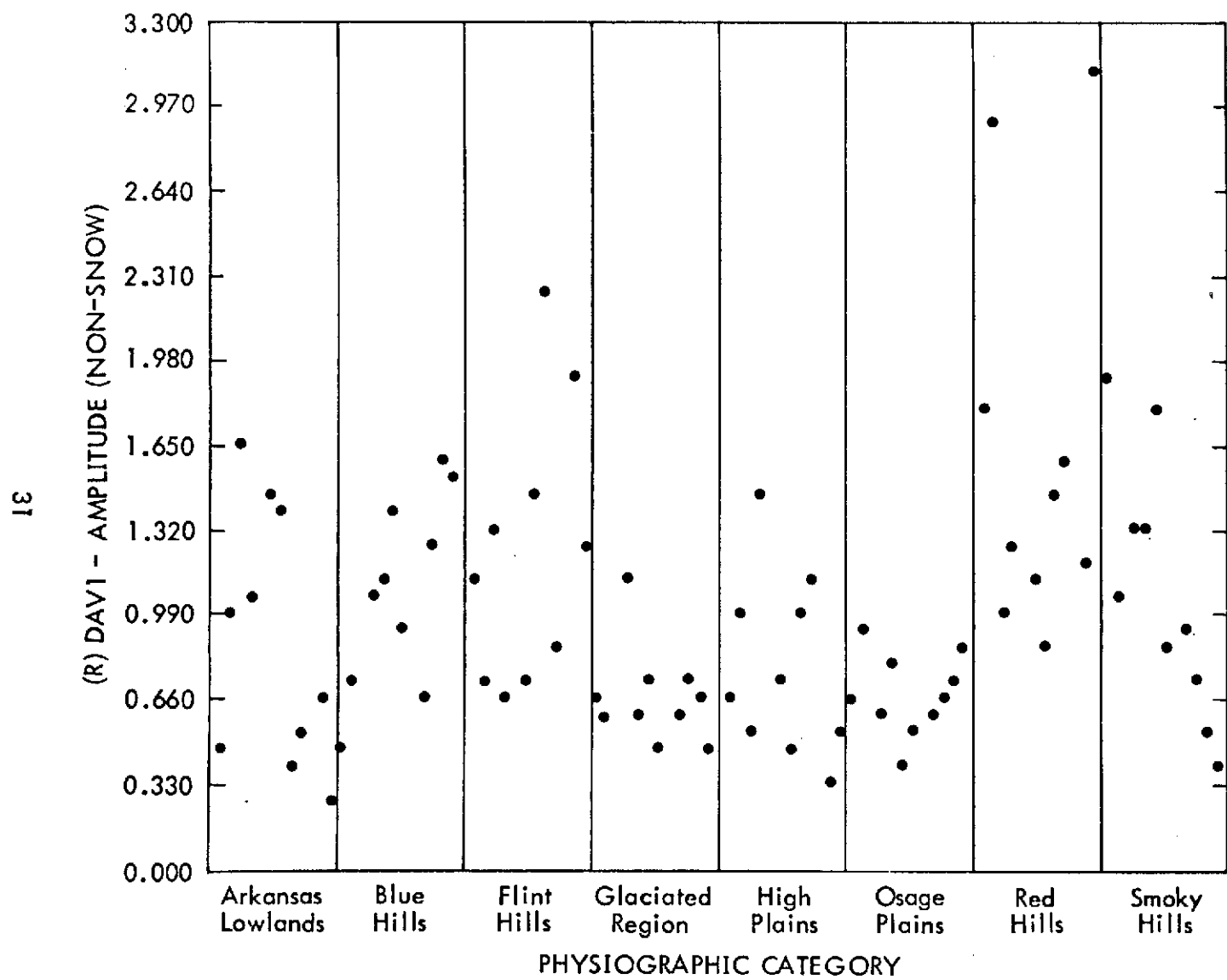


Figure 17. Parameter Plot Using the Parameter (R) DAV1.

4.2 Physiographic Patterns Identified

Decision boundaries may be inserted into the parameter plots shown in the last section based on the distribution of the amplitudes of the parameter. If there is a clear relationship between the amplitude of the parameter and the physiographic characteristics of the sample area, then this decision boundary will discriminate between 2 large-scale physiographic ground patterns.

This was done for the parameter labelled SLOPE 2 and the results of this scheme are shown in Figure 18. As mentioned previously, SLOPE 2 is merely the slope of the regression line for the modified spatial frequency curve for the frequencies in band 2. As can be seen from the plot showing the parameter SLOPE 2 (Figure 15), a decision boundary may be inserted at approximately zero slope ($\pm .001$) which effectively separates the various categories. Sample areas from categories of relatively large high frequency content (Flint Hills, Red Hills, Smoky Hills) yield a positive slope, whereas sample areas from the other categories yield a negative value of this parameter.

This identification experiment resulted in an accuracy of 92.5% with only 6 incorrect identifications based on the original categorization of the sample areas. Sample sites represented by a square were identified as belonging to the category comprising the Flint Hills, Red Hills, and Smoky Hills; sample sites represented by a triangle were identified as belonging to the category comprising the Arkansas River Valley Lowlands, High Plains, Osage Plains, Blue Hills, and the Glaciated Region.

Figure 19 illustrates how a further classification based upon the original physiographic regions can be made. The figure shows a scattergram made by plotting values of the parameters DARAN 2 versus values of SLOPE 2. Values on this graph corresponding to sample areas in the Red Hills, Flint Hills, and Smoky Hills are designated by an open circle; values corresponding to sample areas in the Blue Hills are designated by a black circle; values corresponding to sample areas in the Glaciated Region and Osage Plains are designated by an open square; and values corresponding to sample areas in the High Plains and the Arkansas River Valley Lowlands Regions of Kansas are designated by a black square.

The categories listed above each appear to be distributed in separate portions of the graph. It is apparent that we may insert decision boundaries into this graph to separate the various categories as was done in the one-dimensional case

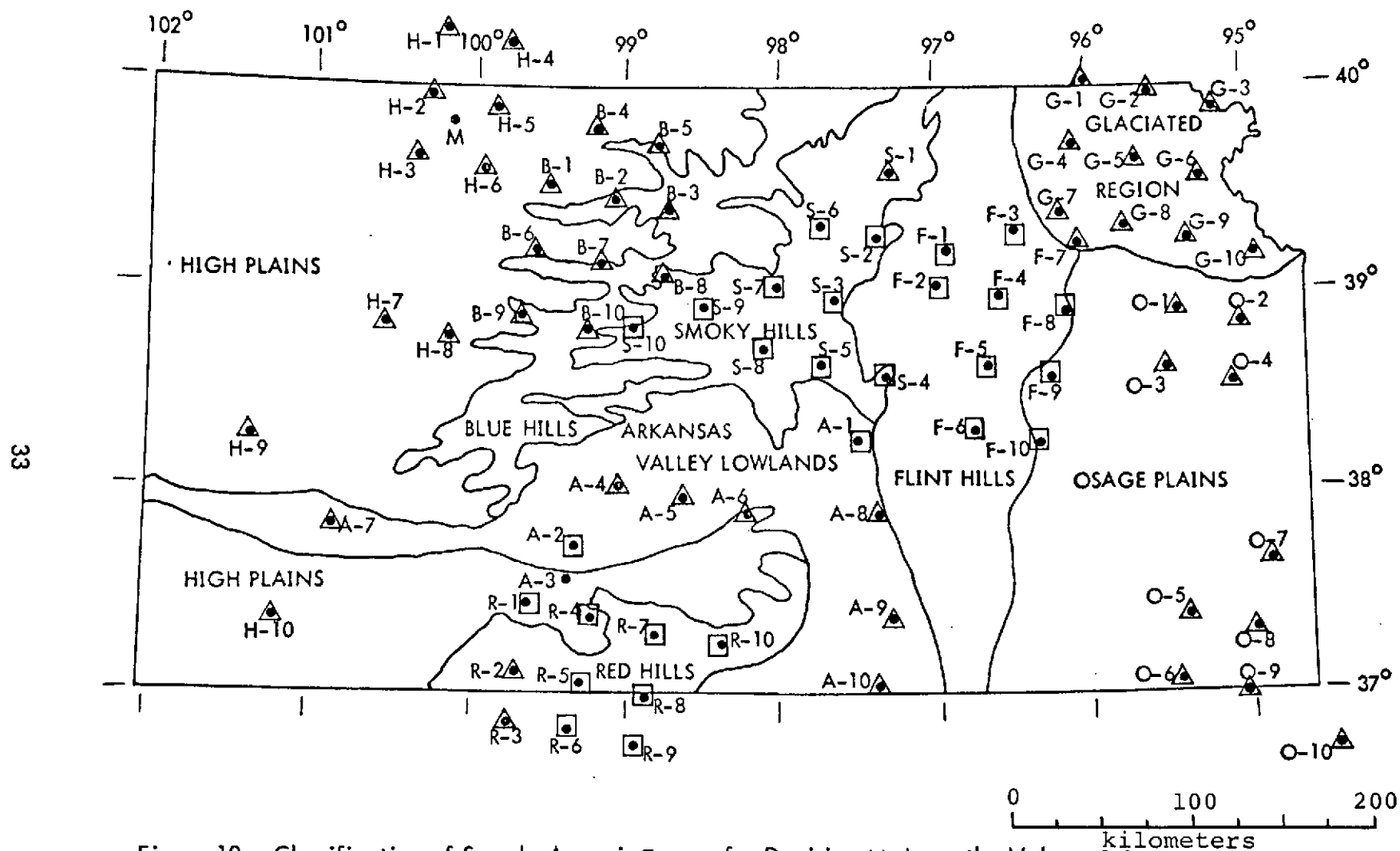


Figure 18. Classification of Sample Areas in Terms of a Decision Made on the Value of the Parameter SLOPE2 for Each Sample Area.

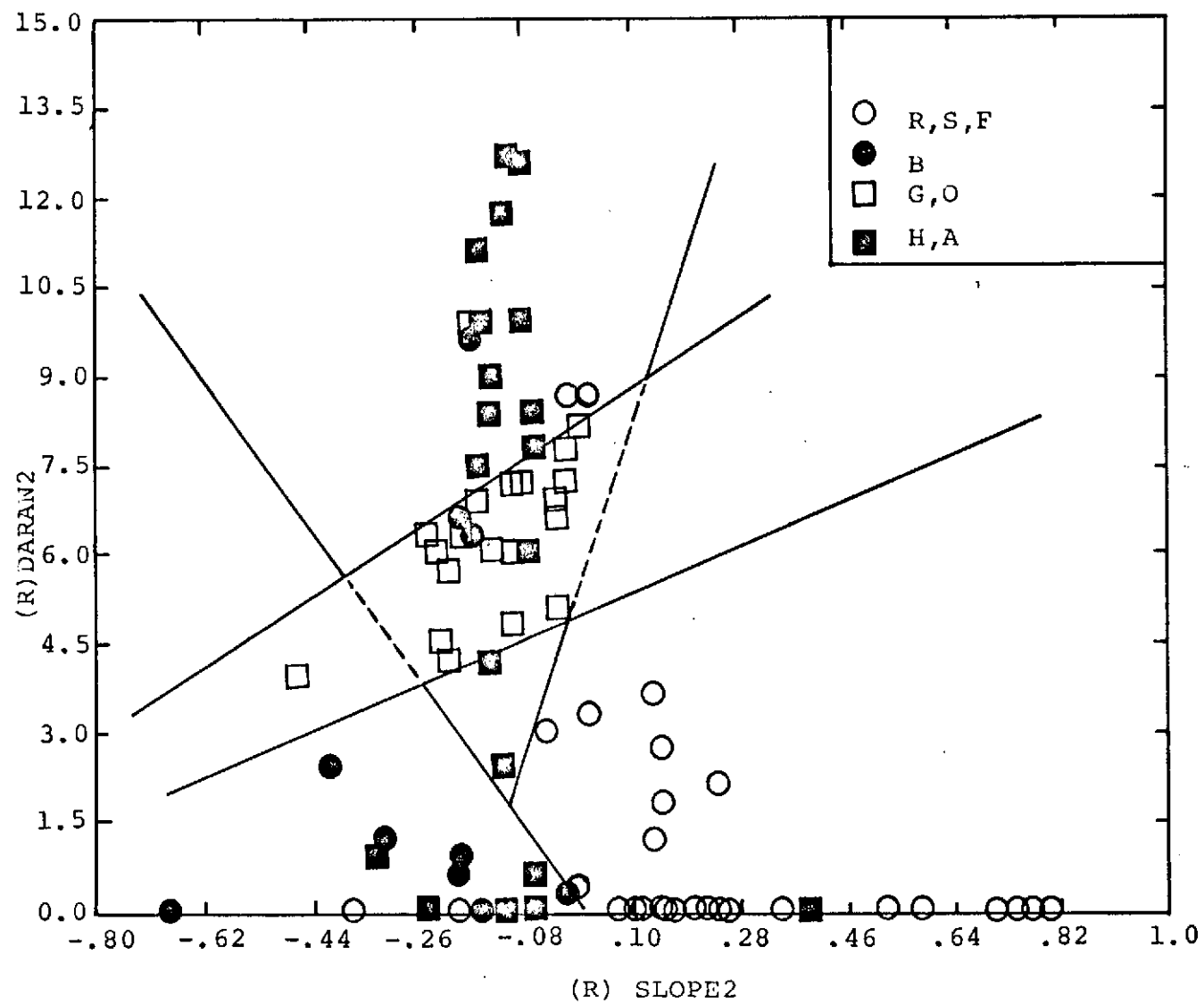


Figure 19. Scattergram obtained using the parameters SLOPE2 and DARAN2.

shown previously. If we now define a region for each category in terms of these boundaries, we may determine how accurately these two parameters classify each sample area. This was done and the results of this classification are shown in Table 1. The overall accuracy in terms of a correct identification for each sample area is 80% for this case.

The sample areas are shown in Figure 20 with respect to their identification based on Figure 19. Figure 20 shows that although the sample areas were identified with an accuracy of only 80%, the sample areas appear to be clustered in Kansas in terms of their identified categories. For instance, A-4, A-5, and A-6 are classified with the Blue Hills to the north, and H-8 is classified with the Blue Hills immediately to the east of it. The category designation in Figure 20 is the same as in Figure 19.

Various algorithms exist to effect the classification made here automatically. One such scheme given in Fukunaga (1972) uses a regression type algorithm to assign samples to various categories. A program based on this algorithm and developed by Haralick and Shanmugan (1973) was used in an attempt to classify the sample areas, but we had only limited success with this program because of the relatively small number of samples used here.

TABLE 1.

Result of Classification of Sample Areas Based on Figure 19.

CATEGORY	HIT	MISSED	TOTAL SAMPLES	% ACCURACY
R,S,F	25	5	30	83
B	7	3	10	70
G,O	19	1	20	95
H,A	13	7	20	65
TOTAL	64	16	80	80

R - RED HILLS
 S - SMOKY HILLS
 F - FLINT HILLS

B - BLUE HILLS

G - GLACIATED REGION
 O - OSAGE PLAINS

H - HIGH PLAINS
 A - ARKANSAS
 LOWLANDS

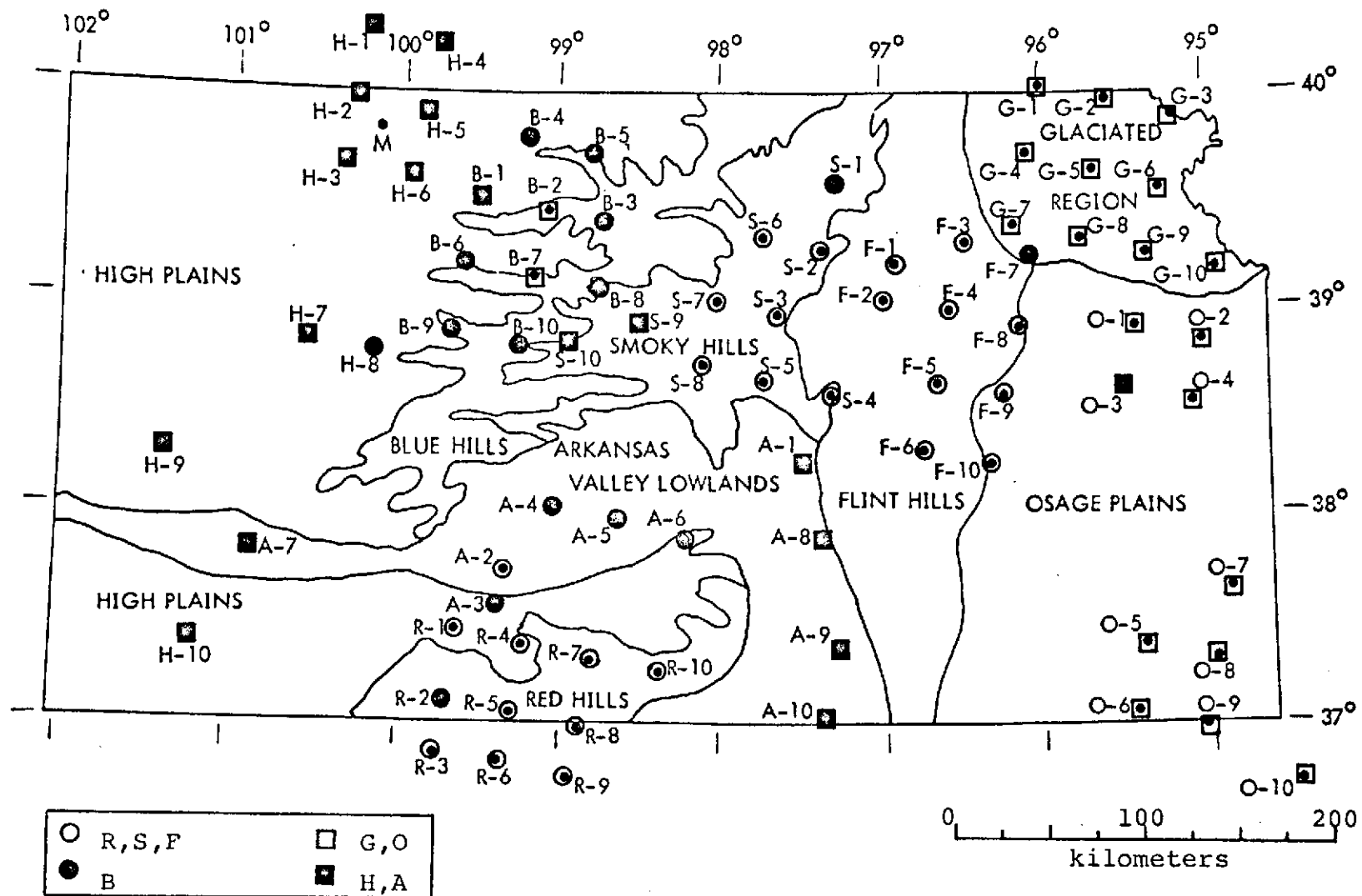
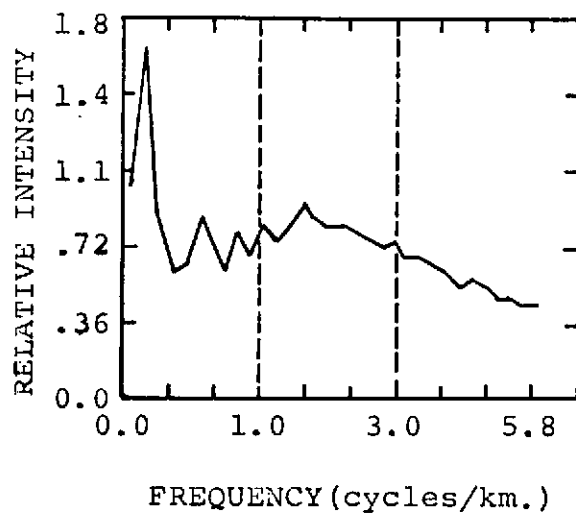


Figure 20. Classification of Sample Areas Based on Figure 19.

4.3 Information Content of Frequency Bands

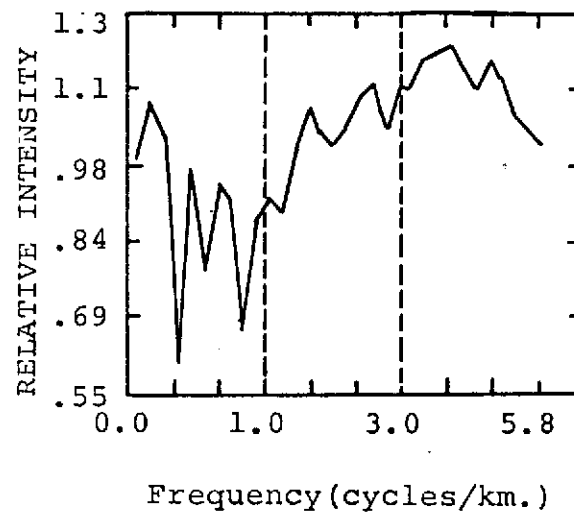
In an effort to determine the band of spatial frequencies that contain the most information with respect to discriminating between physiographic categories, an additional experiment was performed. Data from the optical processing of some of the ERTS sample areas were obtained using a reduced spatial frequency scale. The scale in the transform plane was changed in order to obtain spatial frequency information on frequencies between 2.8 and 5.8 cycles/km.

Two of the reduced scale modified spatial frequency curves obtained in this experiment are shown in Figure 21 (a), and (b). These curves are from the same sample areas shown in Figures 9, and 12. The three frequency bands over which parameters are calculated are also illustrated in this figure. Band 1 contains frequencies between 0.0 and 0.9 cycles/km; band 2 contains frequencies between 1.1 and 2.8 cycles/km; and band 3 contains frequencies between 3.1 and 5.8 cycles/km. The feature parameters described previously were obtained for the additional frequency band (band 3). The parameters calculated for band 3 appeared to provide approximately the same information with respect to discriminating between the physiographic categories for some of the parameters. In general band 3 did not work as well as band 2 in separating the categories.



G-5

(a)



F-6

(b)

Figure 21. Examples of the Modified Spatial Frequency Curves Showing the Curves in All Three Frequency Bands for Sample Areas G-5, F-6.

5.0 CONCLUSIONS

The evidence presented in this paper establishes that optical data processing of ERTS-1 images can be used very successfully in identifying large-scale ground patterns in Kansas. An important point is that the sample areas that were used in this investigation are not uniform. That is they do not display merely one dominant characteristic. Because each sample area is approximately 37 kilometers in diameter, the terrain may vary substantially within each sample area. Even given this 'noise' associated with the sample areas, this method works very well to identify the sample areas in terms of the original physiographic categories.

The manual interpretation of the spatial frequency and orientational curves shown here for one sample area and presented for all the sample areas in Ulaby et al. (1973), demonstrated that this method of analysis can provide an unbiased means of evaluating the orientations and natures of stream patterns and other features apparent in the image.

The band of frequencies between 1.1 and 2.8 cycles/km appears to contain most of the information useful in discriminating between the various physiographic categories. The nature of the information contained in frequencies below 1.1 cycles/km is not apparent with respect to classifying the categories; the nature of the information in the frequencies from 3.1 to 5.8 cycles/km appears to discriminate between categories almost as well as the band from 1.1 to 2.8 cycles/km but only for certain parameters. Sample pattern orientational information is not as useful in discriminating between categories as the spatial frequency information.

Snow cover suppresses patterns due to agriculture and vegetation while enhancing the topography. Such topographic enhancement aids manual geologic interpretation and stream pattern analysis. However, the processing of the sample areas with snow-cover did not provide any help in terms of identifying the sample areas. In fact, snow cover seemed to obscure the information useful in discriminating between categories. It is possible that the snow cover obscured the contributions due to the high frequency information in the band from 1.2 to 2.8 cycles/km.

It is important to note here that the method of analysis used in this investigation is very general. The same methods and algorithms could be applied in general to various other image analysis or categorization problems. The method of analysis shown here is image independent and could be completely automated.

APPENDIX A. Optical Processor Equations

The Fourier transforming property of a simple lens system was demonstrated in section 2.1. Now we consider the more general case used in this investigation and illustrated in Figure 5 and again here in Figure A-1, where a point source at O is imaged by a single positive lens at a point O' in a plane at U_4 .

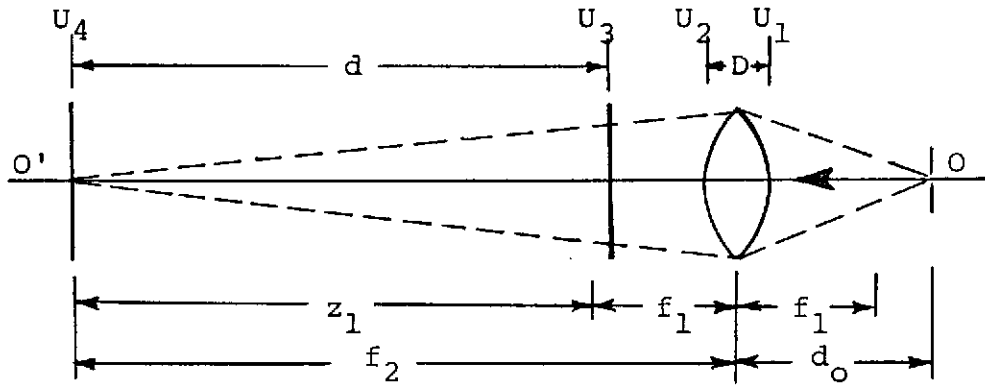


Figure A-1. Configuration Assumed for the Derivation of Equation A-6.

The transparency in this case is placed behind the lens. We will show here that this general configuration also demonstrates the Fourier transforming property and illustrate the origin of Equation 1.

The complex distribution in front of the lens in plane U_1 , using a paraxial approximation to a spherical wave, is:

$$U_1(x_1, y_1) = A \exp(jk d_0) \exp\left[j \frac{k}{2d_0} (x_1^2 + y_1^2)\right] \quad (A-1)$$

The distribution behind the lens in plane U_2 given the

distribution in U_1 is (from eqs. 5-2, 5-10, pp. 78-81 in Goodman):

$$\begin{aligned} U_2(x_2, y_2) &= A \exp(jkd_0) \exp\left[j\frac{k}{2d_0}(x_1^2 + y_1^2)\right] \\ &\quad \times \exp(jknD) \exp\left[-j\frac{k}{2f}(x_2^2 + y_2^2)\right] \quad (A-2) \\ &= A \exp(jkd_0) \exp(jknD) \exp\left[-j\frac{k}{2}\left(\frac{1}{f} - \frac{1}{d}\right)(x_2^2 + y_2^2)\right] \end{aligned}$$

where $x_2 = x_1$; $y_2 = y_1$; from the thin lens approximation.

Now let: $A \exp(jkd_0) \exp(jknD) = A'$; and use the lens law

$$\frac{1}{f_1} - \frac{1}{d_0} = \frac{1}{f_2} = \frac{1}{f_1 + z_1}$$

to obtain:

$$U_2(x_2, y_2) = A' \exp\left[-j\frac{k}{2f_2}(x_2^2 + y_2^2)\right] \quad (A-3)$$

This equation represents the complex distribution behind a lens of focal length f_2 illuminated by a normally incident plane wave of amplitude A' .

At plane U_3 , the transparency, represented by a complex transmittance function t_0 , is multiplied by the incident distribution to obtain (Goodman p. 88):

$$\begin{aligned} U_3(x_3, y_3) &= t_0(x_3, y_3) A' \frac{f_2}{d} P\left(\frac{f_2}{d} x_3, \frac{f_2}{d} y_3\right) \\ &\quad \times \exp\left[-j\frac{k}{2d}(x_3^2 + y_3^2)\right] \quad (A-4) \end{aligned}$$

where the distribution is scaled appropriately and the factor $P\left(\frac{f_2}{d} x_3, \frac{f_2}{d} y_3\right)$ represents the area on the image transparency illuminated due to the projection of the pupil function of the lens down the cone of light rays onto the transparency.

If Fresnel diffraction is assumed from the object plane U_3 to U_4 , then (Goodman p. 60):

$$\begin{aligned}
U_4(x_4, y_4) &= \frac{\exp(jkd)}{j\lambda d} \exp\left[j\frac{k}{2d}(x_4^2 + y_4^2)\right] \\
&\times \int_{-\infty}^{\infty} \int_{-\infty}^{\infty} U_3(x_3, y_3) \exp\left[j\frac{k}{2d}(x_3^2 + y_3^2)\right] \\
&\times \exp\left[-j\frac{2\pi}{\lambda d}(x_4 x_3 + y_4 y_3)\right] dx_3 dy_3 \quad (A-5)
\end{aligned}$$

Finally, substituting eq. (A-4) into eq. (A-5):

$$\begin{aligned}
U_4(x_4, y_4) &= \frac{A'}{j\lambda d} \exp\left[j\frac{k}{2d}(x_4^2 + y_4^2)\right] \frac{f_z}{d} \\
&\times \int_{-\infty}^{\infty} \int_{-\infty}^{\infty} t_o(x_3, y_3) P\left(\frac{f_z}{d}x_3, \frac{f_z}{d}y_3\right) \\
&\times \exp\left[-j\frac{2\pi}{\lambda d}(x_3 x_4 + y_3 y_4)\right] dx_3 dy_3 \quad (A-6)
\end{aligned}$$

where a constant phase factor has been dropped.

If the quadratic phase factor is neglected, eq. (A-6) states that the distribution in plane U_4 is merely the Fourier transform of the transmission function describing that portion of the transparency illuminated by the projected light rays and scaled appropriately. Thus, this general lens system also demonstrates an inherent Fourier transforming property. Equation 2 is obtained from eq. (A-6) by noting that this Fourier transform has a scale factor associated with it based on the geometry of the system. That is, the transform must be evaluated at frequencies $f_x = \frac{x_4}{\lambda d}$, $f_y = \frac{y_4}{\lambda d}$, or combining these we obtain $s = \frac{r}{d\lambda}$ which is equation 2, where s equals the spatial frequency at a radius r from the optical axis in the transform plane.

APPENDIX B. Equipment

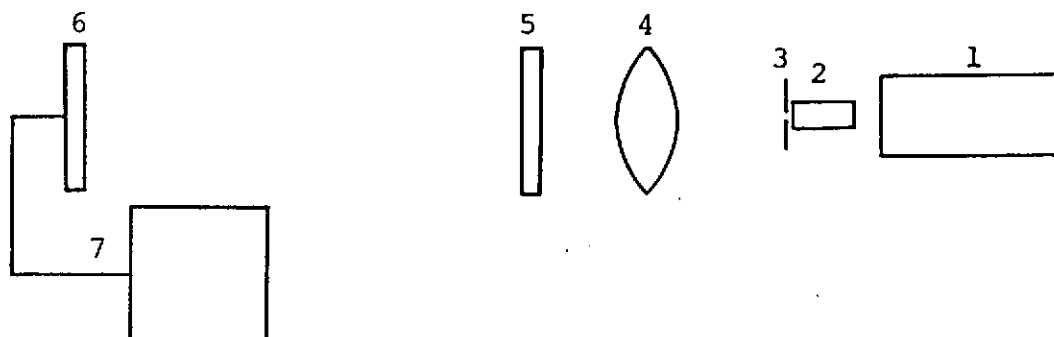


Figure B-1. Optical Processing Equipment.

- | | |
|-------------------------|-------------------------------------------------------------------------------------------------------------------------------------------------------------------------------------------------------------------------------------------------------------------------------------------------------------------------------------|
| 1. Laser | Spectra-Physics Model 134 HeNe laser. Output power--4mw. Wavelength--6328 Angstroms. |
| 2. Microscope objective | } Acts as spatial filter and beam expander. Output is an Airy pattern. |
| 3. 25 micron pinhole | |
| 4. Lens | The lens (focal length = 16.8 cm) images the point source formed at 3 in the plane at 6. The lens iris diaphragm is adjusted to pass the central lobe of the Airy pattern formed at 3. |
| 5. Image holder | The image is inserted and moved in this plane to select the desired sample area. |
| 6,7. DPSU | Recognition Systems Incorporated Diffraction Pattern Sampling Unit (DPSU). 64 element photodiode array at 6, (see Figure 6), samples the diffraction pattern formed in this plane. The unit at 7 amplifies the output from each photodiode. Each photodiode can be switched into the circuit and the resultant amplitude displayed. |

TABLE B-1

Average Radii of Photodetector Annular Rings(see Fig.6)

ring no.	r (mils)
1	0.0
2	8.0
3	14.3
4	21.8
5	30.3
6	40.0
7	50.6
8	62.2
9	74.8
10	88.3
11	103.
12	118.
13	135.
14	152.
15	170.
16	189.
17	209.
18	229.
19	251.
20	273.
21	296.
22	321.
23	346.
24	372.
25	398.
26	426.
27	454.
28	484.
29	514.
30	545.
31	577.
32	610.

r = Average radius from center
of detector.

(These are the average distances from the center of the detector array for each element in thousandths of an inch as calculated from the manufacturers data.)

APPENDIX C. Geology and Physiography of Kansas

(From Ulaby et al. (1973))

Kansas lies within the Stable Interior, a large geologic province of North America occupying most of the region between the Appalachians and the Rocky Mountains. This area has suffered little in the way of intense tectonic activity since early Cambrian sediments were first deposited approximately 600 million years ago. The area which is now Kansas was the site of shallow seas during a good portion of this period. The result has been the formation and preservation of sedimentary formations (sandstones, shales, and limestones) which cover the much older pre-Cambrian basement rocks. The total thickness of these sedimentary rocks is nowhere more than 9500'. This sedimentary cover is thin when compared to sedimentary thicknesses in other parts of the country where sedimentary basins may be 20,000' to 30,000' deep.

The sedimentary formations in Kansas are relatively thin and exhibit a slight but persistent westward dip at the surface. The present day streams and rivers of the state flow in a generally eastward direction from the piedmont of the Rocky Mountains to the Missouri and Mississippi Rivers. This reflects the uplift and eastward tilting of much of the state which occurred with the formation of the Rocky Mountains. Thus the surface elevation of the state increases from the eastern border to the western boundary ranging from less than 800' to more than 4,000'. In traveling in a westward direction across the state, one not only gains elevation but crosses the outcrops of progressively younger sedimentary rocks. Because of the westward dip of the rock units and the subsequent erosion, they are arranged in a staircase fashion with each upward step representing a younger sedimentary unit.

The lithologic makeup of a rock unit, its structural attitude and the weathering forces operating upon it determine the landforms that will form in the area of its outcrop. Because of the westward dip of sedimentary rocks in Kansas, and their layer-cake arrangement, much of the surface of the state is characterized by a series of eastward facing escarpments or cuestas. These features occur where a relatively resistant unit (such as a limestone) crops out. Such a unit tends to produce a landform having a steep eastern face and gentle western slope. This gentle back slope often extends across the outcrop of an overlying, less resistant unit

(such as a shale) to the base of the escarpment formed by the next resistant unit. These escarpments are dissected by the erosive effects of the many eastward flowing streams and as a result have an irregular appearance on a map or aerial photo. But on a larger scale they maintain a general north-south orientation which is at right angles to the prevailing dip direction of the exposed rock units.

Lithologic differences are responsible for the various physiographic regions generally recognized in Kansas which are shown in Figure 1. In the eastern part of the state are the Osage Plains which are made up of a series of eastward-facing escarpments formed by outcrops of Pennsylvanian limestones and shales. The Flint Hills are actually a large escarpment formed by outcrops of a series of chert-bearing Permian limestones that are very resistant to erosion. The Dakota sandstone outcrops (Cretaceous) form the Smoky Hills upland in the North Central part of the state. Likewise, the Blue Hills are formed by outcrops of Upper Cretaceous limestones and chalks.

Beyond the Blue Hills lie the High Plains which are formed by the accumulation of sediments derived from the erosion of the Rocky Mountains to the west. Numerous aggrading streams swept eastward during the Tertiary carrying and depositing sand and gravel and forming a vast outwash plain, that is today the present land surface. Even younger deposits occur in the various prairies and lowlands associated with the Arkansas River. Some of these areas are covered with wind blown sand in the form of dunes, both stabilized and active. In the south-central part of the state are the Red Hills or Cimarron breaks marking the border of the High Plains in the vicinity of the Cimarron River, which together with its tributaries eroded into the red Permian siltstones and shales which underlie the High Plains in that area. The extreme northeast corner of the state was occupied by the Kansan glacier during the Pleistocene. As a result, the landscape was resculptured to some extent and the area was covered to varying depths by glacial deposits.

STRUCTURAL GEOLOGY

The structure of Kansas is subtle for the most part, seldom being dramatically expressed on the surface. This should be kept in mind when considering remote sensors as tools in mapping the geology or structure of Kansas.

Although faulting and folding are not intense or widespread in Kansas, joints are. According to Billings (1942), "Joints may be defined as divisional planes or surfaces that divide rocks and along which there has been no visible movement parallel to the plane or surface". As Merriam (1963, p. 254) states, "Little work has been done on jointing in Kansas, although the joints are extensively developed". Ward (K.G.S. Bulletin 191, pt. 2) in 1968 did a study of joint patterns in the Southern Flint Hills and he concluded, among other things, that the joint patterns measured showed a close correlation to regional tilting and may have been produced at the time of the tilting. He also states that, "The present drainage patterns appear to be closely related to and may be determined by the joint pattern", (Ward 1968, p. 21). He adds, like Merriam before him that "more work concerning midcontinent joint systems is justified" (Ward 1968, p. 21).

Stream patterns have long been known by geologists to reflect the underlying structures, faulting, folding and jointing. Such deformation tends to rupture competent formations creating planes of weakness along which weathering activities are accelerated and through which streams have a tendency to flow, taking advantage of the destructive work already done for them. Thus, by studying topographic patterns in an area, insight can be gained concerning the geologic structure.

Many studies have been performed by geologist using aerial photographs as an aid in structural analysis. Kelley (1960) mapped regional fracture systems for a large area of the Colorado Plateau using aerial photography. Boyer and McOwen (1964) working in Texas established a relationship between fracture patterns observed on the ground and linear features on aerial photographs. Likewise, in the Appalachian Plateau, Lattman (1958) established a correlation between bed rock joint systems and linear features on aerial photographs. These studies and many others like them involve the visual detection, measurements, and evaluation of linear features or lineaments. Such studies are limited by the interpreter's ability to detect lineaments and may be handicapped by a biased evaluation of their significant. Spatial frequency analysis may provide a means of detecting and measuring linear features on imagery which would not ordinarily be detected by visual means. In addition, such analysis would not be guided by any preordained knowledge of the geologic structure, and the results would be unbiased. The small scale of the imagery used in this study negates the detection of actual fractures or joints on the ground. However, the linear features associated with stream traces and topographic alignments can be detected and will provide most of the information concerning geologic structure.

LAND USE

Land-use in Kansas is predominately devoted to agriculture. However, the type of agriculture practiced varies across the state, due to climate, soil, landform, and availability of water. Agricultural land-use can be correlated fairly well with the physiographic regions of Figure 1. The area east of the Flint Hills, namely the Osage Plains and the Glaciated Region, is characterized by mixed farming of the corn belt type, with generally small fields and pastures and a variety of crops grown including corn, soybeans, milo, etc. Hay is an important crop in some areas of the southern part of this area and stock farming is a common practice. To the west lies the Flint Hills region with its areas of bluestem prairie. It is predominately a ranching area specializing in finishing out transient cattle brought in from western and southwestern ranges. The Blue Hills and Smoky Hills are also large cattle grazing regions, especially in the rougher areas where cultivation is impractical. In this same regard the Red Hills region of the south-central part of the state is also an important ranching area. Much of the arable area in the western two-thirds of the state is devoted to the raising of wheat, with the most extensive wheat growing areas in the level and fertile lowlands associated with the Arkansas River. Much wheat is also grown on the level uplands of the High Plains and in favorable areas in the Smoky Hills and Blue Hills. However, dry farming is in common practice in the western part of Kansas, where rainfall is deficient. Dry farming involves practices designed to catch and conserve the available moisture. Toward this end, dry farming often involves the fallowing of fields for one or two years in order to build up a reserve of soil moisture. Thus in any given year in the western part of the state, a sizable portion of the cultivated land will be free of planted crops. Much of the High Plains is also devoted to the grazing of cattle especially the rougher lands along streams. The southern High Plains of Kansas is an important grain sorghum growing area.

Irrigation is important in parts of western Kansas. The largest and most extensive area of irrigation is centered around Garden City, reaching from Scott City southward into Meade County and westward along the Arkansas River. This area is underlain by a sedimentary basin containing thick deposits of the Tertiary Ogallala formation. This formation is largely sand and gravels derived from the Rocky Mountain in Tertiary time. Its porous and permeable nature make it an excellent aquifer (water yielding formation) and it feeds the many irrigation wells in this

area. Several crops are grown here including corn, wheat, soybeans, alfalfa, and sugar beets. Other irrigated areas in the High Plains regions also rely on the ground water stored in the Ogallala. The more recent deposits of alluvial material in the valley of the Arkansas River are also important aquifers. The tell-tale signs of irrigation on areal photos are the circular fields produced by pivot sprinkler systems. The circular fields are quite large (1/2 mile in diameter) and are discernible on ERTS imagery as well.

The Arkansas River valley also contains areas of sand hills. In most of these areas, the sand hills or dunes are stabilized and covered by natural vegetation. Some areas are active however with dunes in formation and smaller areas of wind erosion called blowouts. Because of the rolling topography of these sand hill tracts, many are uncultivated and used as grazing areas.

On an area basis, non-agricultural land use is, of course, secondary in Kansas. The remaining land area is largely tied up in cities and towns, reservoirs and their surrounding management areas, military installations, wildlife refuges and mining areas. These land uses are largely self-explanatory. However, land use related to mining activity requires further elaboration.

Among the minerals and rocks mined in the state are lead, zinc, coal gypsum, salt, volcanic ash, limestone, sand, gravel, and clay. In addition, the state is an important oil and gas producer. Of these activities; salt, lead, and zinc mining is performed under ground. Most of the other products are mined by quarrying operations that are generally small in areal extent. The exception is the procurement of coal which is done by strip mining. Large areas in southeast Kansas bear the effects of strip mining in the form of long parallel mounds of dirt and rock which represent the overburden removed to reach the underlying coal seam. Lakes occupy many of these abandoned strip pits today and are used as a recreational resource in the area. The reclamation of strip mined land is an important issue in Kansas where the practice is in use and being expanded to new areas.

GEOLOGIC PATTERNS ON ERTS IMAGERY

In satellite imagery of an area such as Kansas with low relief, subtle geologic structure and extensive land-use, the geologic ground pattern that is most apparent is that caused by stream patterns. Pattern and frequency of streams

are important indicators of the rock-type upon which they are developed. In addition, they are strongly influenced by geologic structure. Spatial frequency analysis of ERTS imagery lends itself to the study of drainage patterns by detecting those patterns which display a preferred orientation or spacing. Curves that result from such analysis may contain "signatures" that are attributable to basic geologic parameters. In addition, insight may be gained concerning structural trends by detecting stream orientations that may be influenced by joints and other structures. Such insight would be useful since little knowledge is available concerning joint trends in Kansas and their significance.

Use of spatial frequency analysis in the study of stream patterns should be guided by a knowledge of the manner in which stream patterns are expressed on ERTS imagery and how this expression varies from place to place in the state as a result of changing rock-type, landuse, climate and natural vegetation.

In Kansas, stream courses are generally expressed on ERTS imagery in four different ways:

1. Riparian Vegetation

In the eastern half of the state are many stream valleys that support denser and higher stands of vegetation than do the surrounding uplands. Cottonwoods, willows and other trees and shrubs which require large amounts of water thrive near streams that are perennial or contain water during much of the year. Such streams are relatively easy to identify on ERTS-1 images with the MSS5 band giving the best expression. On this band, riparian vegetation generally appears much darker than surrounding fields and grasslands. In the western half of the state the increased dryness restricts this type of vegetation to only the major perennial streams such as the Arkansas River and the lower Smoky Hill.

2. Pure Topographic Enhancement

Several areas in the state are largely uncultivated. For the most part, these are ranching areas that are covered with both natural and introduced grasses. Trees and shrubs are generally lacking even along streams in many of these areas. The absence of distractive patterns caused by fields and gross vegetation differences permit the enhancement of topography by differential illumination of slopes of varying orientation. This expression can be found on images covering the Kansas Flint Hills, as well as the Red Hills, Smoky Hills and dissected regions adjacent to larger streams in the High Plains.

Topographic Enhancement of drainage patterns has a much broader application in the winter at times of deep snow cover. The snow has the effect of giving the landscape more uniform reflecting properties by masking over areas of different crop and vegetation type. As a result, slope orientation becomes more critical in determining the amount of sunlight reflected to the ERTS-sensors. The lower sun angle in the winter serves to further enhance the topography. Thus an area in which stream patterns are not normally discernible may display them fully when snow-covered.

3. Land-Use

Differing land-use between stream valleys and uplands can often accentuate stream patterns. This can come about in a number of ways. One involves bottom land cultivation in an area of upland grazing and occurs in association with the major streams in the Flint Hills and other hilly areas, where the level fertile flood plains offer the most desirable farming areas.

Another method by which land-use reflects stream patterns occurs in the western part of the state and is the opposite of the previously mentioned method. It is best displayed in the High Plains and dissected High Plains area where stream valleys are often rough and lack flood plains. In this case the level upland areas offer the most ideal conditions for cultivation. The valleys which are usually too rough or rocky for farming are used as pasture.

4. Direct Stream Expression

In some situations, the actual stream beds can be delineated on ERTS imagery. This occurs in two ways. In the eastern portion of the state the larger streams usually contain water throughout the year and can often be discerned on the MSS 6 and MSS 7 bands of ERTS imagery due to the low return of infrared energy from water bodies. Thus the larger streams are often dark in comparison to the surrounding countryside.

In a different manner, actual stream beds in the western and south-central part of the state are also expressed on ERTS imagery. In this situation, it is the dry stream beds which give a distinctive appearance. These dry streams are choked with sand, which highly reflects energy in the visible region and produces a bright appearance on MSS 4 and MSS 5 images which contrast well with the less bright appearance of surrounding fields and vegetation.

APPENDIX D. Fortran IV Programs

This appendix contains a listing of the Fortran IV programs used in the analysis of the data obtained from the optical processing system. The programs are labelled and arranged in the following order:

Program:

1. DPSU DATA CALIBRATION PROGRAM

Calibrates and normalizes the data obtained from the DPSU. Prints, punches, and plots the resultant data.

2. DPSU DATA ANALYSIS--PARAMETERS/WEDGE CURVES

Uses wedge data from program 1 to obtain parameters which describe features in the wedge data curve. Calculates these parameters for 4 sectors: wedges (1-8), (9-16), (17-24), (25-32). Prints and punches resultant data.

3. DPSU DATA ANALYSIS--SPATIAL FREQUENCY CURVES MODIFIED

Calculates a modified spatial frequency curve by dividing each frequency curve obtained from program 1 (point-by-point) by average frequency curve. Prints punches, and plots resultant data.

4. DPSU DATA ANALYSIS--PARAMETERS/SPATIAL FREQUENCY CURVES

Uses modified spatial frequency curve data obtained from program 3 to calculate parameters which describe features in frequency curve. Calculates these parameters for two frequency bands. Prints and punches the resultant data.

```

C          DPSL DATA CALIBRATION PROGRAM ( 05/25/73 )
C
C
C          PROGRAM
C          INPUT--D(I,J) (DATA FROM DPSU)
C                  --N,(TOTAL NO. OF DATA SETS)
C                  N1,(NO. OF FIRST DATA SET)
C          OUTPUT--CALIBRATED RING,WEDGE DATA--PRINTED,PUNCHED,
C                  PLOTTED
C
C          LABELS
C          L= NO. OF DATA SET
C          A= RING AREAS ( 32 VALUES )
C          F= CALIBRATION FACTORS ( 32 VALUES )--(AREA/SENSITIVITY
C              CORRECTION FOR WEDGES )
C
C          DIMENSION D(70,64),B(64,70),DN(64),DL(64),D1P(33),D2P(33),X(33),
C          1A(32),F(32),DI(64),DT(64),KK(200),LL(11)
C          **DIMENSIONS FOR D, B, SET HERE FOR 70 DATA SETS**
C          DATA A/80.8,99.8,202.,344.,548.,707.,1050.,1440.,1920.,2510.,3150.
C          1,3910.,4770.,5730.,6850.,8060.,9390.,10900.,12400.,14200.,16100.,1
C          28100.,20200.,22500.,25100.,27500.,30500.,33400.,36700.,40500.,4330
C          30.,46400./,
C          4F/      1.052,1.070,1.043,1.058,1.061,1.064,1.064,1.054,1.049,1.0
C          545,1.037,1.017,1.008,1.008,1.014,1.017,1.008,1.006,1.000,1.011,1.0
C          625,1.031,1.037,1.034,1.034,1.040,1.034,1.034,1.037,1.040,1.037,1.0
C          737/
C
C          READ(5,100)N,N1
C
C          **READ DATA USING FREE FORMAT SUBROUTINE**
C
C          CALL FFMT (5,8)

```



```

      DO 1 J=1,64
      DO 1 I=1,N
1    D(I,J)=9(J,I)
C
      DO 40 K=1,11
40   LL(K)=K
      DO 4 K=1,33
4    X(K)=K
      DO 2 I=1,N
C
C    **RING DATA COMPUTATION**
C
      D1=D(I,1)/A(1)
      DO 3 J=1,32
      DN(J)=D(I,J)/(D1*A(J))
      DT(J)=DN(J)*10.**10
      DL(J)=ALOG10(DT(J))/10.
3    CONTINUE
C
C    **WEDGE DATA COMPUTATION**
C
      D2=D(I,33)*F(1)
      DO 29 J=33,64
      DI(J)=D(I,J)*F(J-32)
      IF(DI(J).GT.D2)D2=DI(J)
29   CONTINUE
      DO 50 J=33,64
50   DN(J)=DI(J)/D2
C
C    VALUES FOR PLOTS PUT INTO D1P , D2P
C
      D1P(33)=0.4
      D2P(33)=0.4
      DO 7 J=1,32
      D1P(J)=DL(J)

```

```

7 D2P(J)=DN(J+32)
  L=I+N1-1
  KK(L)=L

```

C
C
C

```

**PUNCH, PRINT, PLOT, CALIBRATED DATA **

```

```

WRITE(43,102) KK(L),(DN(J),J=1,6),LL(1)
WRITE(43,102) KK(L),(DN(J),J=7,12),LL(2)
WRITE(43,102) KK(L),(DN(J),J=13,18),LL(3)
WRITE(43,102) KK(L),(DN(J),J=19,24),LL(4)
WRITE(43,102) KK(L),(DN(J),J=25,30),LL(5)
WRITE(43,102) KK(L),(DN(J),J=31,36),LL(6)
WRITE(43,102) KK(L),(DN(J),J=37,42),LL(7)
WRITE(43,102) KK(L),(DN(J),J=43,48),LL(8)
WRITE(43,102) KK(L),(DN(J),J=49,54),LL(9)
WRITE(43,102) KK(L),(DN(J),J=55,60),LL(10)
WRITE(43,112) KK(L),(DN(J),J=61,64),LL(11)
WRITE(6,113) KK(L)
WRITE (6,114)
WRITE (6,101) (D(I,J),J=1,64)
WRITE(6,104)
WRITE(6,105)
WRITE (6,106) ((J,DN(J),DL(J),J,DN(J+32)),J=1,32)
WRITE(6,115)
WRITE(6,116)
CALL PLT2(2,X,D1P,33,X,D2P,33)
WRITE(6,107)
WRITE (6,108)
WRITE(6,110)
WRITE (6,111)

```

```

2 CONTINUE

```

```

100 FORMAT(1X,I4,I5)

```

```

101 FORMAT (6X,8F8.3)

```

```

102 FORMAT (1X,I3,2X,6E11.4,6X,I2)

```

```

104 FORMAT(1H0,5X,49HR=NORMALIZED RING VALUE, W=NORMALIZED WEDGE VALUE

```


DPSU DATA ANALYSIS -- PARAMETERS/WEDGE CURVES

PROGRAM

INPUT-- DN(N), CALIBRATED, NORMALIZED, RING AND WEDGE DATA

OUTPUT-- W1-W8, W9-W16, W17-W24, W25-W32, OVERALL

1) AVERAGE (DAV)

2) RMS DEVIATION FROM AVERAGE (RMSD)

3) AREA

(*) ABOVE/BELOW AVE)--(+) AREA=(AREA), (-) AREA=(ARAN)

4) DATA POINTS ABOVE AVE) (PAKS)

5) NUMBER OF 'PEAKS' IN REGION (PEAKS)

(NOTE-- REGION 1=(W1-W8), REGION 2=(W9-W16), REGION 3=(W17-W24),

REGION 4=(W25-W32))

```

DIMENSION DN(64, 80), DIFF(32, 80), KK(80), DAV( 80), DAV1( 80),
1 DAV2( 80), DAV3( 80), DAV4( 80), AREA( 80), AREA1( 80), AREA2( 80),
2 AREA3( 80), AREA4( 80), ARAN1( 80), ARAN2( 80), ARAN3( 80), ARAN4( 80),
3 PAKS( 80), PAK1( 80), PAK2( 80), PAK3( 80), PAK4( 80), RMSD( 80),
4 RMSD1( 80), RMSD2( 80), RMSD3( 80), RMSD4( 80), A1(80), PEAK1(80),
5 PEAK2(80), PEAK3(80), PEAK4(80)

```

DATA NO /80/

DO 309 I = 1, NO

READ DATA

READ(5,100) (DN(N,I), N=1,60)

100 FORMAT(6X, 6E11.4)

READ(5,113) (KK(I), (DN(N,I), N=61,64))

113 FORMAT(1X,13,2X,4E11.4)

DATA AVERAGE CALCULATION

SUM1=0.00

SUM2=0.00

SUM3=0.00

SUM4=0.00

DO 21 N=33,40

21 SUM1=SUM1 + DN(N,I)

DO 22 N=41,48

22 SUM2=SUM2 + DN(N,I)

DO 23 N=49,56

23 SUM3=SUM3 + DN(N,I)

DO 24 N=57,64

24 SUM4=SUM4 + DN(N,I)

SUM=SUM1 + SUM2 + SUM3 + SUM4

DAV(I) = SUM/32.0

DAV1(I) = SUM1/8.00

DAV2(I) = SUM2/8.00

DAV3(I) = SUM3/8.00

DAV4(I) = SUM4/8.00

DATA AREA/DATA PEAK CALCULATION

AREA(I) = 0.00

AREA1(I) = 0.00

AREA2(I) = 0.00

AREA3(I) = 0.00

AREA4(I) = 0.00

ARAN1(I) = 0.00

ARAN2(I) = 0.00

ARAN3(I) = 0.00

```

ARAN4(I) = 0.00
THRS = DAV(I)
PAK1(I) = 0.0
PAK2(I) = 0.0
PAK3(I) = 0.0
PAK4(I) = 0.0
PEAK1(I) = 0.0
PEAK2(I) = 0.0
PEAK3(I) = 0.0
PEAK4(I) = 0.0

```

C
C

```

SUMSQ = 0.00
DO 30 N = 33,40
DIFF = DN(N,I) - DAV1(I)
SQDIF = DIFF * DIFF
SUMSQ = SUMSQ + SQDIF
IF(DN(N,I).GT.THRS) PAK1(I) = PAK1(I) + 1.0
DIFF(N,I) = DN(N,I) - DAV(I)
IF(DIFF(N,I)) 31,32,32
31 ARAN1(I) = ARAN1(I) - DIFF(N,I)
DIFF(N,I) = 0.00
32 AREA1(I) = AREA1(I) + DIFF(I,I)
Y = DN(N,I)
Y2 = DN(N-1,I)
IF(N.EQ.33) Y2 = DN(N+1,I)
IF(N.EQ.64) GO TO 35
Y1 = DN(N+1,I)
GO TO 37
35 Y1 = Y2
37 IF((Y.GT.Y1).AND.(Y.GT.Y2)) PEAK1(I) = PEAK1(I) + 1.0
30 CONTINUE
SUMAV = SUMSQ / 8.00
RMSD1(I) = SQRT(SUMAV)

```

C

```

SUMSQ = 0.00
DO 40 N = 41,48
DIFF = DN(N,1) - DAV2(I)
SQDIF = DIFF * DIFF
SUMSQ = SUMSQ + SQDIF
IF(DN(N,1).GT.THRS) PAK2(I) = PAK2(I) + 1.0
DIFF(N,1) = DN(N,1) - DAV(I)
IF(DIFF(N,1)) 42,43,43
42 ARAN2(I) = ARAN2(I) - DIFF(N,1)
DIFF(N,1) = 0.00
43 AREA2(I) = AREA2(I) + DIFF(I,1)
Y = DN(N,1)
Y2 = DN(N-1,1)
IF(N.EQ.33) Y2 = DN(N+1,1)
IF(N.EQ.64) GO TO 45
Y1 = DN(N+1,1)
GO TO 47
45 Y1 = Y2
47 IF((Y.GT.Y1).AND.(Y.GT.Y2)) PAK2(I) = PAK2(I) + 1.0
40 CONTINUE
SUMAV = SUMSQ / 8.00
RMSD2(I) = SQRT(SUMAV)

```

C

```

SUMSQ = 0.00
DO 50 N = 49,56
DIFF = DN(N,1) - DAV3(I)
SQDIF = DIFF * DIFF
SUMSQ = SUMSQ + SQDIF
IF(DN(N,1).GT.THRS) PAK3(I) = PAK3(I) + 1.0
DIFF(N,1) = DN(N,1) - DAV(I)
IF(DIFF(N,1)) 52,53,53
52 ARAN3(I) = ARAN3(I) - DIFF(N,1)
DIFF(N,1) = 0.00

```

```

53 AREA3(I) = AREA3(I) + DIFF(I,I)
   Y = DN(I,I)
   Y2 = DN(N-1,I)
   IF(N.EQ.33) Y2 = DN(N+1,I)
   IF(N.EQ.64) GO TO 55
   Y1 = DN(N+1,I)
   GO TO 57
55 Y1 = Y2
57 IF((Y.GT.Y1).AND.(Y.GT.Y2)) PEAK3(I) = PEAK3(I) + 1.0
50 CONTINUE
   SUMAV = SUMSQ / 8.00
   RMSD3(I) = SQRT(SUMAV)

```

C

```

   SUMSQ = 0.00
   DO 60 N = 57,64
   DIFF = DN(N,I) - DAV4(I)
   SQDIF = DIFF * DIFF
   SUMSQ = SUMSQ + SQDIF
   IF(DN(N,I).GT.THRS) PAK4(I) = PAK4(I) + 1.0
   DIFF(N,I) = DN(N,I) - DAV(I)
   IF (DIFF(N,I)) 62,63,63
62 ARAN4(I) = ARAN4(I) - DIFF(N,I)
   DIFF(N,I) = 0.00
63 AREA4(I) = AREA4(I) + DIFF(N,I)
   Y = DN(N,I)
   Y2 = DN(N-1,I)
   IF(N.EQ.33) Y2 = DN(N+1,I)
   IF(N.EQ.64) GO TO 65
   Y1 = DN(N+1,I)
   GO TO 67
65 Y1 = Y2
67 IF((Y.GT.Y1).AND.(Y.GT.Y2)) PEAK4(I) = PEAK4(I) + 1.0
60 CONTINUE
   SUMAV = SUMSQ / 8.00
   RMSD4(I) = SQRT(SUMAV)

```


C

AREA(I) = AREA1(I) + AREA2(I) + AREA3(I) + AREA4(I)

PAKS(I) = PAK1(I) + PAK2(I) + PAK3(I) + PAK4(I)

SUMSQ = 0.00

DO 39 N = 33,64

SQDIF = DIFF(N,I) * DIFF(I,I)

SUMSQ = SUMSQ + SQDIF

39 CONTINUE

SUMAV = SUMSQ/32.0

RMSD(I) = SQRT(SUMAV)

309 CONTINUE

C

C

WRITE(6,101)

WRITE(6,102) (KK(I), DAV(I), DAV1(I), DAV2(I), DAV3(I), DAV4(I),

I=1,NO)

WRITE(6,103)

WRITE(6,104) (KK(I), AREA(I), AREA1(I), AREA2(I), AREA3(I), AREA4(I),

I=1,NO)

WRITE(6,105)

WRITE(6,106) (KK(I), ARAN1(I), ARAN2(I), ARAN3(I), ARAN4(I), I=1,NO)

WRITE(6,107)

WRITE(6,108) (KK(I), PAKS(I), PAK1(I), PAK2(I), PAK3(I), PAK4(I),

I=1,NO)

WRITE(6,109)

WRITE(6,110) (KK(I), RMSD(I), RMSD1(I), RMSD2(I), RMSD3(I), RMSD4(I),

I=1,NO)

WRITE(6,121)

WRITE(6,123) (KK(I), PEAK1(I), PEAK2(I), PEAK3(I), PEAK4(I),

I=1,NO)

C

WRITE(43,401) (KK(I), DAV(I), DAV1(I), DAV2(I), DAV3(I), DAV4(I),

RMSD(I), RMSD1(I), RMSD2(I), RMSD3(I), RMSD4(I), I=1,NO)

401 FORMAT(15,10F7.3)

WRITE(43,402) (KK(I), AREA(I), AREA1(I), AREA2(I), AREA3(I), AREA4(I),

ARAN1(I), ARAN2(I), ARAN3(I), ARAN4(I), I=1,NO)

```

402 FORMAT(15,9F7.3)
WRITE(43,402) (KK(I),PAKS(I),PAK1(I),PAK2(I),PAK3(I),PAK4(I),
1      PEAK1(I),PEAK2(I),PEAK3(I),PEAK4(I),I=1,NQ)
C
101 FORMAT('1',10X,'AVE',12X,'AVE1',11X,'AVE2',11X,'AVE3',11X,'AVE4')
102 FORMAT('0',I3,F11.3,F15.3,F15.3,F15.3,F15.3)
103 FORMAT('1',10X,'AREA TOTAL',5X,'AREA 1',9X,'AREA 2',9X
1,'AREA 3',9X,'AREA 4')
104 FORMAT('0',I3,F11.3,F15.3,F15.3,F15.3,F15.3)
105 FORMAT('1',25X,'(-)AREA 1',6X,'(-)AREA 2',6X,'(-)AREA 3',6X,
1,'(-)AREA 4')
106 FORMAT('0',I3,11X,F15.3,F15.3,F15.3,F15.3)
107 FORMAT('1',10X,'PAKS',10X,'PAK1',10X,'PAK2',10X,'PAK3',10X,
1,'PAK4')
108 FORMAT('0',I3,F11.3,F15.3,F15.3,F15.3,F15.3)
109 FORMAT('1',10X,'RMS',12X,'RMS 1',10X,'RMS 2',10X,'RMS 3',10X,
1,'RMS 4')
110 FORMAT('0',I3,F11.3,F15.3,F15.3,F15.3,F15.3)
121 FORMAT('1',25X,
1'PEAK1',10X,'PEAK2',10X,'PEAK3',10X,
1'PEAK4')
123 FORMAT('0',I3,11X,F15.3,F15.3,F15.3,F15.3)
C *****
C *****
C *****
C *****
C *****
C *****
STOP
END

```

C DPSU DATA ANALYSIS-- SPATIAL FREQUENCY CURVES-MODIFIED

C PROGRAM

C 1) OBTAINS PL1 = D1/AVE , , PL2 = D1/TH
C 2) PLOTS PL1

C LABELS

C D1 = CALIBRATED , NORMALIZED DATA FROM DPSU
C TH = CALIBRATED , NORMALIZED , CORRECTED DATA FROM DPSU
C (NO IMAGE INPUT)
C AVE = AVERAGE DATA SET OBTAINED FROM ALL SETS
C DN = CALIBRATED , NORMALIZED , CORRECTED , DATA FROM DPSU

C INPUT -- DN

C OUTPUT -- PL1,PL2,PL1 PLOTTED

C DIMENSION DN(64),D1(80,32), PL1(33),PL2(32),TH(32),
C 1AVE(33),SUM1(32),KK(148),X(33),LL(3),AVED(33)

C DATA TH/ 1.00E-0,7.93E-2,4.20E-3,3.73E-4,
C 18.77E-5,

C 23.82E-5,2.27E-5,1.45E-5,1.01E-5,7.50E-6,7.06E-6,1.04E-5,2.39E-5,
C 32.16E-5,1.70E-5,1.31E-5,9.71E-6,8.04E-6,5.92E-6,4.52E-6,3.21E-6,
C 42.29E-6,1.71E-6,1.25E-6,8.82E-7,6.28E-7,5.01E-7,4.01E-7,3.45E-7,
C 52.97E-7,2.58E-7,2.51E-7/

C DATA NO/4/

C

C INITIALIZE SUM1(N)

C

C DO 301 N = 1,32

C 301 SUM1(N) = 0.00

C DO 910 1 = 1,NO

C

C **READ DATA **

C

 READ(5,100) (DN(N),N = 1,60)

100 FORMAT(6X,6E11.4)

 READ(5,113) KK(I),(DN(N),N = 61,64)

113 FORMAT(1X,13,2X,4E11.4)

C

C ** COMPUTE DATA SET AVERAGE **

C

 DO 201 N = 1,32

 D1(I,N) = DN(N)

201 SUM1(N) = SUM1(N) + D1(I,N)

910 CONTINUE

 DO 801 N = 1,32

 AVE(N) = SUM1(N)/FLOAT(NO)

 AVEM = AVE(N)*10.**10

 AVED(N) = ALOG10(AVEM)/10.0

801 CONTINUE

 AVED(33) = AVED(32)

 WRITE(6,504)

504 FORMAT('1','DATA AVERAGE')

 WRITE(6,503)((N,AVE(N),AVED(N)),N=1,32)

503 FORMAT(' ',6X,13,9X,E11.4,E11.4)

C

C ** COMPUTE PL1,,PL2 **

C

 DO 901 I = 1,NO

 DO 310 N = 1,32

 PL1(N) = D1(I,N)/AVE(N)

 PL2(N) = D1(I,N)/TH(N)

310 CONTINUE

 PL1(33) = PL1(32)

C

C ** PRINT ,, PLOT ,, PUNCH **

C

 WRITE(6,701) KK(I)

```

701 FORMAT('1','DATA SET NO.',1X,13)
WRITE(6,501)
501 FORMAT('0',8X,'N',10X,'PL1',10X,'PL2')
WRITE(6,502)((N,PL1(N),PL2(N)),N = 1,32)
502 FORMAT(' ',6X,13,6X,F7.3,5X,F7.2)
DO 300 K = 1,33
300 X(K) = K
CALL PLT2(1,X,PL1,33,X,PL1,33)
WRITE(6,107)
WRITE(6,108)
DO 76 K = 1,3
76 LL(K) = K
WRITE(43,80) KK(I),(PL1(N),N = 1,12),LL(1)
WRITE(43,80) KK(I),(PL1(N),N = 13,24),LL(2)
WRITE(43,82) KK(I),(PL1(N),N = 25,32),LL(3)
80 FORMAT(1X,13,1X,12F6.3,2X,11)
82 FORMAT(1X,13,1X,8F6.3,26X,11)
901 CONTINUE
CALL PLT2(1,X,AVED,33,X,AVED,33)
WRITE(6,107)
WRITE(6,108)
107 FORMAT(11X,'---+---+---+---1---+---+---+---1---+---+---+---1---+---+---+---
1+---1---+---+---+---1---+---+---+---1---+---+---')
108 FORMAT(16X,'2',5X,'4',5X,'6',4X,'8',4X,'10',4X,'12',4X,'14',3X,'16
1',4X,'18',4X,'20',3X,'22',4X,'24',4X,'26',4X,'28',3X,'30',4X,'32')
STOP
END

```

```

C          DPSU DATA ANALYSIS -- PARAMETERS/SPATIAL FREQUENCY CURVES
C
C
C
C
C          PROGRAM ----- MODIFIED
C          INPUT-- DATA(N), DATA FROM MODIFIED SPATIAL FREQUENCY CURVES
C          -- KK(I), DATA SET N1.
C          OUTPUT-- R1-R21, R22-R32, OVERALL
C          1) AVERAGE (DAV)
C          2) RMS DEVIATION FROM AVERAGE (RMSD)
C          3) AREA
C          (*) ABOVE/BELOW AVE.--(+)AREA=(AREA), (-)AREA=(ARAN)
C          (**) ABOVE/BELOW 1.0 --(+)AREA=(DARA), (-)AREA=(DARAN)
C          4) DYNAMIC RANGE--(DYNR)
C          5) SLOPE OF CURVE(R22-R32)--(SLOPE)
C
C          (NOTE-- REGION 1 = (R1-R21), REGION 2 = (R22-R32))
C
C
C          DIMENSION DATA(32), KK(32), DAV(32), DAV1(32), DAV2(32), DIFF(32),
C          1ARAN1(32), ARAN2(32), AREA(32), AREA1(32), AREA2(32), DIFF1(32),
C          2DARAN1(32), DARAN2(32), DARA1(32), DARA2(32), DARA(32), DYNR1(32),
C          3DYNR2(32), DYNR(32), RMSD(32), RMSD1(32), RMSD2(32), SLOPE(32), X(11),
C          4Y(11), A1(32)
C          DATA NO/32/
C          DO 900 I = 1, 40
C
C          ** READ DATA **
C
C          READ(5, 701) (DATA(N), N=1, 24)
C          701 FORMAT(5X, 12F6.3)
C          READ(5, 703) KK(I), (DATA(N), N=25, 32)
C          703 FORMAT(1X, 13, 1X, 8F6.3)
C

```

C ** DATA AVERAGE **

C

SUM1 = 0.00

SUM2 = 0.0

SUM = 0.0

AREA1(I) = 0.00

AREA2(I) = 0.00

ARAN1(I) = 0.00

ARAN2(I) = 0.00

DARA1(I) = 0.00

DARA2(I) = 0.00

DARAN1(I) = 0.00

DARAN2(I) = 0.00

DO 21 N=1,21

21 SUM1 = SUM1 + DATA(N)

DO 22 N =22,32

22 SUM2 = SUM2 + DATA(N)

SUM = SUM1 + SUM2

DAV(I) = SUM/32.0

DAV1(I) = SUM1/21.0

DAV2(I) = SUM2/11.0

C

C

C

**REGION 1 (R1-R21)--AREA OF CURVE,RMS,DYNR

HI1 = DATA(1)

XLO1 = DATA(1)

SUMSQ1 = 0.00

DO 31 N=1,21

DIFFE = DATA(N) - DAV1(I)

SQDIF = DIFFE * DIFFE

SUMSQ1 = SUMSQ1 + SQDIF

DIFF(N) = DATA(N) - DAV(I)

IF(DIFF(N)) 32,33,33

32 ARAN1(I) = ARAN1(I) - DIFF(N)

DIFF(N) = 0.0

33 AREA1(I) = AREA1(I) + DIFF(I)

```

      DIFF1(N) = DATA(N) - 1.00
      IF(DIFF1(N)) 35,36,36
35  DARAN1(I) = DARAN1(I) - DIFF1(N)
      DIFF1(N) = 0.0
36  DARA1(I) = DARA1(I) + DIFF1(N)

```

C

```

      IF(DATA(N).GT.H11) H11 = DATA(N)
      IF(DATA(N).LT.XL01)XL01 = DATA(N)
31  CONTINUE
      DYNR1(I) = H11 - XL01
      SUMAV = SUMSQ1/21.0
      RMSD1(I) = SQRT(SUMAV)

```

C

C

C

```

      **REGION 2 (R22-R32)-- AREA OF CURVE,RMS,DYNR**

```

```

      H12 = DATA(22)
      XL02 = DATA(22)
      SUMSQ2 = 0.00
      DO 41 N = 22,32
      DIFFE = DATA(N) - DAV2(I)
      SQDIF = DIFFE * DIFFE
      SUMSQ2 = SUMSQ2 + SQDIF
      DIFF(N) = DATA(N) - DAV(I)
      IF(DIFF(N)) 42,43,43
42  ARAN2(I) = ARAN2(I) - DIFF(N)
      DIFF(N) = 0.0
43  AREA2(I) = AREA2(I) + DIFF(N)
      DIFF1(N) = DATA(N) - 1.00
      IF(DIFF1(N)) 45,46,46
45  DARAN2(I) = DARAN2(I) - DIFF1(N)
      DIFF1(N) = 0.00
46  DARA2(I) = DARA2(I) + DIFF1(N)

```

C

C


```

IF(DATA(N).GT.HI2) HI2 = DATA(N)
IF(DATA(N).LT.XLO2) XLO2 = DATA(N)

```

C

```

M = N - 21
Y(M) = DATA(N)

```

```

41 CONTINUE
DYNR2(I) = HI2 - XLO2
SUMAV = SUMSQ2 / 11.0
RMSD2(I) = SQRT(SUMAV)

```

C

C

```

DARA(I) = DARA1(I) + DARA2(I)
AREA(I) = AREA1(I) + AREA2(I)
SUMSQ = 0.00
SUMSQ = SUMSQ1 + SUMSQ2
SUMAV = SUMSQ/32.0
RMSD(I) = SQRT(SUMAV)

```

C

```

HI = HI1
IF(HI2.GE.HI1) HI = HI2
XLO = XLO1
IF(XLO2.LE.XLO1) XLO = XLO2
DYNR(I) = HI - XLO

```

C

```

DO 801 J= 1,11
801 X(J) = FLOAT(J)/10.0
CALL SLOP(X,Y,11,C,SLOPE,COEF)
SLOPE(I) = SLOPE

```

```

900 CONTINUE

```

```

WRITE(6,101)
WRITE(6,102) (KK(I),DAV(I),DAV1(I),DAV2(I),I=1,NO)
WRITE(6,103)
WRITE(6,104) (KK(I),AREA(I),AREA1(I),AREA2(I),ARAN1(I),ARAN2(I),
1I = 1,NO)
WRITE(6,105)
WRITE(6,106) (KK(I),DARA(I),DARA1(I),DARA2(I),DARAN1(I),DARAN2(I),

```

```

      11 = 1,NO)
      WRITE(6,111)
      WRITE(6,112) (KK(I),RMSD(I),RMSD1(I),RMSD2(I),I=1,NO)
      WRITE(6,107)
      WRITE(6,108) (KK(I),DYNR(I),DYNR1(I),DYNR2(I),I=1,NO)
      WRITE(6,109)
      WRITE (6,110)(KK(I),SLOPE(I),I=1,NO)
      WRITE(43,201)(KK(I),DAV(I),DAV1(I),DAV2(I),SLOPE(I),I=1,NO)
201  FORMAT(15,4F7.3)
      WRITE(43,203)(KK(I),AREA(I),AREA1(I),AREA2(I),ARAN1(I),ARAN2(I),
1DARA(I),DARA1(I),DARA2(I),DARAN1(I),DARAN2(I),I=1,NO)
203  FORMAT(15,10F7.3)
      WRITE(43,205)(KK(I),RMSD(I),RMSD1(I),RMSD2(I),DYNR(I),DYNR1(I),
1DYNR2(I),I=1,NO)
205  FORMAT(15,6F7.3)
C
C
101  FORMAT('1',10X,'AVE',12X,'AVE1',11X,'AVE2')
102  FORMAT('0',I3,F11.3,F15.3,F15.3)
103  FORMAT('1',10X,'AREA TOTAL',5X,'AREA 1',9X,'AREA 2',9X,'(-)AREA 1'
1,6X,'(-)AREA 2')
104  FORMAT('0',I3,F11.3,F15.3,F15.3,F15.3,F15.3)
105  FORMAT('1',10X,'1.0 AREA TOTAL',2X,'AREA 1',8X,'AREA 2',9X,
1'(-)AREA1',6X,'(-)AREA 2')
106  FORMAT('0',I3,F11.3,F15.3,F15.3,F15.3,F15.3)
107  FORMAT('1',10X,'DYNR',11X,'DYNR1',10X,'DYNR2')
108  FORMAT('0',I3,F11.4,F15.3,F15.3)
109  FORMAT('1',10X,'SLOPE OF CURVE-(R10-R32)')
110  FORMAT('0',I3,F10.5)
111  FORMAT('1',10X,'RMS',12X,'RMS 1',10X,'RMS 2')
112  FORMAT('0',I3,F11.4,F15.4,F15.4)
C
C
      STOP
      END

```

SUBROUTINE SLOP (X,Y,N,C,SLOPE,COEF)

DIMENSION X(1),Y(1)

XN=N

XONE=0.

YONE=0.

XSQAR=0.

XY=0.

DO 5 K=1,N

XSQAR=XSQAR+X(K)*X(K)

XONE=XONE+X(K)

YONE=YONE+Y(K)

XY=XY+X(K)*Y(K)

5 CONTINUE

DENOM=XONE*XONE-XN*XSQAR

SLOPE=(XONE*YONE-XY*XN)/DENOM

C=(XY*XONE-YONE*XSQAR)/DENOM

ANUM=0.

ADEN=0.

XAV=0.

YAV=0.

XN=N

DO 8 I=1,N

XAV=XAV+X(I)

YAV=YAV+Y(I)

8 CONTINUE

XAV=XAV/XN

YAV=YAV/XN

DO 9 I=1,N

ANUM=ANUM+(Y(I)-YAV)*(Y(I)-YAV)

ADEN=ADEN+(X(I)-XAV)*(X(I)-XAV)

9 CONTINUE

COEF=SLOPE*SQRT(ADEN/ANUM)

WRITE(6,7) C,SLOPE,COEF

7 FORMAT(3F10.3)

RETURN

END

REFERENCES

- Andrews, Harry C., et al., (1972), "Image Processing by Digital Computer," IEEE Spectrum, July, 1972.
- Billings, M. P., (1942), Structural Geology, Prentice-Hall, Inc., Engelwood Cliffs, New Jersey.
- Born, M., and E. Wolf, (1959), Principles of Optics, Pergamon Press, New York.
- Boyer, R. E., and J. E. McQueen, (1964), "Comparison of Mapped Rock Fractures and Airphoto Linear Features," Photogrammetric Engineering, vol. 30, pp. 630-635.
- Davis, J. C., and F. W. Preston, (1972), "Optical Processing: An Alternative to Digital Computing", The Geological Society of America, Inc. Special Paper 146, 1972.
- Fukunaga, K., (1972), Introduction to Statistical Pattern Recognition, Academic Press, New York.
- Goodman, J. W., (1968), Introduction to Fourier Optics, McGraw-Hill Book Co., New York.
- Gramenopoulos, Nicholas, (1973), "Terrain Type Recognition Using ERTS-1 MSS Images," ERTS-1 Symposium, March 5-9, 1973, New Carrollton, Maryland.
- Haralick, R. M., K. Shanmugan, (1973), "Computer Classification of Reservoir Sandstones", IEEE Trans. on Geoscience Electronics, vol. GE-11, No. 4, Oct. 1973.
- Kelley, V. C. and J. N. Clinton, (1960), "Fracture Systems and Tectonic Elements of the Colorado Plateau," University of New Mexico Publication in Geology, no. 6, 104 pp.
- Lattman, L. H. and R. P. Nickelson, (1958), "Photogeologic Fracture Trace Mapping in Appalachian Plateau," Am. Assoc. Petroleum Geologists Bull., vol. 42, pp. 2238-2244.
- Lee, T. C., and D. Gossen, (1971), "Generalized Fourier-Transform Holography and its Applications", Applied Optics, Vol. 10, No. 4, April 1971.
- Lendaris, G. G. and G. L. Stanley, (1969), "Diffraction-Pattern Sampling for Automatic Pattern Recognition," Seminar Proceedings, Pattern Recognition Studies, Society of Photo-Optical Instrumentation Engineers, June 9-10, 1969, New York.
- McCauley, J. R., et al., (1974), "Stream Pattern Analysis Using Optical Processing of ERTS Imagery of Kansas," Modern Geology, (in Press).

REFERENCES (Continued)

- McCullagh, M. J., and J. C. Davis, (1972), "Optical Analysis of Two-Dimensional Patterns", Annals of the Association of American Geographers, vol. 62, No. 4, Dec., 1972.
- Merriam, D. F., (1963), "The Geologic History of Kansas, "Kansas Geological Survey Bulletin 162.
- Parrent, G. B. Jr., and B. J. Thompson, (1969), Physical Optics Notebook, Society of Photo-Optical Instrumentation Engineers.
- Pincus, H. J., and Dobrin, M. B., (1966), "Geological Applications of Optical Data Processing", Jour. Geophys. Research, v. 71, p. 4861-4869.
- Preston, Kendall, (1972), Coherent Optical Computers, McGraw-Hill Book Co., New York.
- Read, A. A., and R. F. Cannata (1974), "Coherent Analysis Enriches Yield From 1-D Data Records", Laser Focus, p. 65, May, 1974.
- Remote Sensing, (1970), National Academy of Sciences, Washington, D. C., p. 310.
- Schoewe, W. H., (1949), "The Geography of Kansas, Pt. 2, Physical Geography," Kansas Acad. Sci. Trans., vol. 52, no. 3, pp. 261-333.
- Shulman, A. R., (1970), Optical Data Processing, John Wiley & Sons Inc., New
- Stanley, G. L., Nienow, W. C., and G. G. Lendaris, (1969), "SARF, An Interactive Signature Analysis Research Facility", AC-DRL Technical Report TR 69-15, Santa Barbara, Calif., March 1969.
- Steckley, Robert C., (1972), "Determination of Paleotectonic Principal Stress Direction, Including Analysis of Joints by Optical Diffraction," U. S. Dept. of Interior, Bureau of Mines, PGH.,PA. 18036, U. S. Govt. Printing Office: 1972-709-309:551.
- Ulaby, F. T. (Principal Investigator), et al., (1973) "Ground Pattern Analysis in the Great Plains," CRES Technical Report 2266-4," Semi-Annual ERTS-1 User Investigation Report," University of Kansas Center for Research, Inc , Lawrence, Kansas, July, 1973. Supported by NASA Contract NAS5-21822.
- Ward, J. R., (1968), "A Study of the Joint Patterns in Gently Dipping Sedimentary Rocks of South-Central Kansas, "Kansas Geological Survey Bulletin 191, Part 2.

CRINC LABORATORIES

Chemical Engineering Low Temperature Laboratory

Remote Sensing Laboratory

Flight Research Laboratory

Chemical Engineering Heat Transfer Laboratory

Nuclear Engineering Laboratory

Environmental Health Engineering Laboratory

Information Processing Laboratory

Water Resources Institute

Technical Transfer Laboratory

Air Pollution Laboratory

Satellite Applications Laboratory

